CATALOGED BY ASTIA
AS AD No. 23120

TECHNICAL REPORT

THERMAL SHOCK ANALYSIS OF SPHERICAL SHAPES

BY

W. B. Crandall and J. Ging

ONR Contract N6-ori-143
NR-032-022

Alfred University

Alfred , New York

January 1, 1954

BEST AVAILABLE COPY

ABSTRACT

A method is described for studying the thermal shock characteristics of a brittle material. An analysis of the thermo-stresses developed in a "homogeneous", "isotropic" solid sphere has led to the formulation of an equation relating the physical properties of the body to the temperature difference causing failure and time to maximum stress in a single cycle unsteady state test. The thermal shock test consists of plunging a sphere at one uniform temperature into a medium at another temperature. If fracture occurs the time to fracture is recorded. A large number of tests are run to determine the temperature difference which causes 50% of the spheres to fracture. The thermal shock relationships were tested using Coors' high alumina body. The physical properties relating to the thermal shock equations were measured, and calculated temperature differences causing failure and times to maximum stress were compared with measured values. Sufficient agreement was found to lend support to the theory.

INTRODUCTION

Thermal shock resistance is that property of a body which enables it to withstand sudden and severe temperature changes without fracturing. This ability to withstand thermal shock depends upon such factors as composition, shape, size, temperature distribution, manner of heating and cooling, and the inherent strength of the body. In many applications, it is important to know how the physical properties of a material will affect its ability to withstand thermal shock. An initial approach to this problem becomes thatof establishing the conditions which will cause the thermal stresses in the body to exceed the breaking strength. When a body is heated or cooled the difference in temperature between the different regions sets up thermal stresses which may be analyzed.

Ceramic materials exhibit relatively poor thermal shock resistance, as compared to metals. This is perhaps the main barrier to the extensive use of refractories in jet-propulsion and rocket engines. Because non-ductile, i.e., brittle ceramic materials, possess many desired properties, such as strength at high temperatures and high melting points, there is considerable interest in the spalling behavior of these materials.

The purpose of this investigation was to determine the thermal shock resistance on heating and cooling a brittle solid sphere and to compare the experimental results with the theoretical equations.

THEORETICAL CONSIDERATIONS

In this paper, the thermal shock resistance of any body is defined as the maximum initial temperature difference between the body and its surroundings which the body can withstand without fracturing. Fracture is assumed to take place when the tensile stress at a point exceeds the strength

of the body.

1. General

The theory of elasticity is contained formally in the linear elastic equations which relate the components of stress (σ_{ik}) to the components of strain (ϵ_{ik}):

$$\sigma_{ik} = \Psi \epsilon_{ik} + \sum_{s} \omega \delta_{ik} \epsilon_{ss} \qquad 1.1$$

where $\delta_{ik} = 1$ when $i = k$, 0 when $i \neq k$ and $s, i, k = 1, 2, 3$

together with a cartesian coordinate system (x_i) for the location of the material points of the body. The constants Ψ and ω characterize the elasticity of the body completely and are related to Young's Modulus and the Modulus of Rigidity. Equation (1.1) is applicable, then, only to homogeneous, isotropic bodies.

That the σ_{ik} are symmetric ($\sigma_{ik} = \sigma_{ki}$) is proved easily by considering the rotational equilibrium of an infinitely small parallelopiped about the coordinate axes. The tensor character of the σ_{ik} is proved from the translational equilibrium of an infinitely small tetrahedron.

The strain components ϵ_{ik} can be defined in terms of the strain metric: Two infinitesimally near material points which initially have coordinate differences dx_i will, after the body is distorted, be separated by a distance:

$$ds^2 = \sum_{ik} (\Delta_{ik} + \epsilon_{ik}) dx_i dx_k \qquad 1.2$$

The symmetry and tensor character of the ϵ_{ik} is easily inferred from the form of eq. (1.2). In the following we shall use the convention of summing over those indices which appear twice in the same term. Thus, e.g., eq. (1.2) can be rewritten:

$$ds^2 = (\Lambda_{ik} + \epsilon_{ik})\, dx_i\, dx_k \qquad 1.2A$$

In general the stress distribution σ_{ik} is not given, but must be calculated from a known distribution of body forces per unit volume and surface forces. Denoting the components of the force per unit volume by X_i, an application of Green's Theorem for surface integrals yields the equilibrium conditions:

$$X_i = \frac{\partial \sigma_{is}}{\partial x_s} \qquad 1.3$$

If the body is initially unstrained the ϵ_{ik} are subjected to the restrictions (compatibility conditions):

$$F_{ikrs} = \epsilon_{ik,lm} + \epsilon_{lm,ik} - \epsilon_{il,km} - \epsilon_{km,il} = 0 \qquad 1.4$$

where the comma (,) denotes partial differentiation with respect to the coordinate whose index follows. The system (1.4) constitutes six algebraically independent equations. The system (1.4), (1.1), (1.3), therefore contains 15 equations in the 12 functions σ_{ik} and ϵ_{ik}. Such a system would in general

be over-determined were it not for the existence of 3 identities connecting the equations. These are indeed given by the three "Bianchi" identities for the $P_{ikl}{}^{m}$:

$$P_{ik}{}^{lm}{}_{,n} + P_{ik}{}^{mn}{}_{,s}{}^{l} + P_{ik}{}^{nl}{}_{,m} = 0 \qquad 1.5$$

The system (1.4), (1.1), (1.3), is therefore complete and not over-determined.

2. The Thermo-Elastic Equations

In case a non-uniform temperature distribution exists in the body, eq. (1.1) must be modified to take into account the distortion of volume elements resulting from the thermal expansions. We replace (1.1) by:

$$\sigma_{ik} = \psi_{\epsilon_{ik}} + \omega\lambda_{ik}\epsilon_{ss} - \Gamma\lambda_{ik}\theta \qquad 2.1$$

where θ is the temperature of the point with coordinate (x_i) in excess of some uniform temperature throughout the body. The constant Γ characterizes the thermal expansion of an unrestrained volume element. From hereon, we assume that the volume and surface forces vanish everywhere, so that we have to solve the system:

$$\sigma_{ik} = \psi_{\epsilon_{ik}} + \omega\lambda_{ik}\epsilon_{ss} - \Gamma\lambda_{ik}\theta \qquad 2.1$$

$$\sigma_{is,s} = 0 \qquad 1.3A$$

$$P_{ikl\,m} = 0 \qquad 1.4A$$

3. **Thermal Stresses in the Sphere**

For a sphere heated symmetrically about its center, it is sufficient to write the ϵ_{ik} in the form:

$$\epsilon_{ik} = B\,\Delta_{ik} + D\,x_i x_k \qquad 3.1$$

where B, D are functions of $r' = \sqrt{x_1^2 + x_2^2 + x_3^2}$ only, to be determined. Instead of determining the functions B, D directly by substitution into the system (2.1), (1.3), (1.4), it is simpler to first write the ϵ_{ik} as:

$$\epsilon_{ik} = \frac{1}{2}(f_{i,k} + f_{k,i}) \qquad 3.2$$

This expression for the ϵ_{ik} satisfies eq. (1.4) identically, as a short calculation will reveal. We can further obtain the required form (3.1) by setting:

$$f_i = g(r')\,x_i \qquad 3.3$$

We have, using eq. (3.2):

$$\epsilon_{ik} = g\,\Delta_{ik} + \left(\frac{g'}{r'}\right) x_i x_k \qquad 3.4$$

By eqs. (2.1) and (1.3) the equilibrium equations reduce to:

$$\frac{d}{dr'}\left[\frac{1}{(r')^2}\frac{d}{dr'}(g\,(r')^3)\right] = \frac{\Gamma}{\psi+\omega}\,\rho' \tag{3.5}$$

and we have

$$g = \frac{\Gamma}{\psi+\omega}\,\frac{1}{(r')^3}\int_0^{r'}\rho(r')^2\,dr' + C_1 + \frac{C_2}{(r')^3} \tag{3.6}$$

In order that g be finite at $r' = 0$, we must put $C_2 = 0$ in the above. Substituting (3.6) into (3.4), we find along the x_1 — axis $(x_1 = r,\ x_2 = x_3 = 0)$

$$\epsilon = 3C_1 + \frac{\Gamma}{\psi+\omega}\,\rho' \tag{3.7}$$

$$\epsilon_{11} = \frac{-2\Gamma}{\psi+\omega}\,\frac{1}{(r')^3}\int_0^{r'}\rho(r')^2\,dr' + \frac{\Gamma\rho}{\psi+\omega} + C_1 \tag{3.8}$$

$$\epsilon_{22} = \frac{\Gamma}{\psi+\omega}\,\frac{1}{(r')^3}\int_0^{r'}\rho(r')^2\,dr' + C_1 \tag{3.9}$$

and

$$\sigma_{11} = -\frac{2\Gamma\psi}{\psi+\omega}\,\frac{1}{(r')^3}\int_0^{r'}\rho(r')^2\,dr' + (\psi+3\omega)\,C_1 \tag{3.10}$$

$$\sigma_{33} = \sigma_{22} = \frac{\psi\Gamma}{\psi+\omega}\,\frac{1}{(r')^3}\int_0^{r'}\rho(r')^2\,dr' - \frac{\psi\Gamma}{\psi+\omega}\,\rho + (\psi+3\omega)C_1 \tag{3.11}$$

at $x_1 = r =$ the radius of the sphere, we must have $\sigma_{11} = 0$. Using (3.10) we find:

$$(\psi + 3\omega) C_1 = \frac{2\Gamma\psi}{\psi+\omega} \frac{1}{r^3} \int_0^r \theta (r')^2 dr' \qquad 3.12$$

Using the notation:

$$\bar{\theta} = \frac{3}{r^3} \int_0^r \theta (r')^2 dr' \qquad 3.13$$

$$\bar{\theta}_{r'} = \frac{3}{(r')^3} \int_0^{r'} \theta (r')^2 dr' \qquad 3.14$$

$$\sigma_{ij}^* = \frac{\psi+\omega}{r^3} \quad \text{[illegible]} \qquad 3.15$$

we can rewrite (3.10), (3.11) as:

$$\sigma_{11}^* = \frac{2}{3} (\bar{\theta} - \bar{\theta}_{r'}) \qquad 3.16$$

$$\sigma_{22}^* = \sigma_{33}^* = \frac{2}{3} \bar{\theta} + \frac{1}{3} \bar{\theta}_{r'} - \theta \qquad 3.17$$

All the other stress components vanish along the x_1 axis. When the temperature distribution in the sphere is known, eqs. (3.10), (3.11) give the complete solution to the problem.

For a sphere heated by radiation at the surface with initial uniform temperature taken at zero, we have:

$$f = \frac{2\beta}{\xi} \sum_{n=1}^{n=\infty} e^{-\psi_n^2 f} \frac{\psi_n^2 + (\beta-1)^2}{\psi_n^2[\psi_n^2 + \beta(\beta-1)]} \sin\psi_n \sin\xi\psi_n \qquad 3.18$$

where β = Biot's Modulus

$\xi = \frac{r'}{r}$

$f = \frac{a\theta'}{r^2}$

a = Thermal Diffusivity

θ' = Time to maximum stress

ψ_n = Are the roots of $\psi_n \cot\psi_n + \beta - 1 = 0$ 3.19

and the temperature of the radiation is taken as $\xi = 1$. If, in the right side of (3.18) $\sin\xi\psi_n$ is written as a Taylor's series expanded about $\xi = 0$, it is seen that only even powers of ξ appear. We can consequently obtain a good approximation for f if we write:

$$f = f_0 - M\xi^2 \qquad 3.20$$

where $M = M(\theta')$ and f_0 = center temperature of sphere.
The boundary condition at $\xi = 1$ is:

$$\frac{\partial f}{\partial \xi} + \beta = 0 \qquad 3.21$$

Substituting this into (3.20), we have:

$$M = \frac{\beta}{2} \qquad 3.22$$

Then (3.20) becomes:

$$\rho = \rho_0 \left(1 - \frac{\beta}{\beta+2} \xi^2\right) \tag{3.23}$$

and

$$\bar{\rho} = \rho_0 \left[1 - \frac{3\beta}{5(\beta+2)}\right] \tag{3.24}$$

Using (3.16), (3.17), we find:

$$\tau_{11}^* = -\frac{2\beta}{5(\beta+2)} \rho_0 \quad \text{at} \quad \xi = 0 \tag{3.25}$$

$$\sigma_{22}^* = \frac{2\beta}{5(\beta+2)} \rho_0 \quad \text{at} \quad \xi = 1 \tag{3.26}$$

To this approximation the maximum stress evidently occurs for ρ_0 close to unity. The maximum stresses are therefore approximately:

$$-\sigma_{11}^{*}{}_{max} = \sigma_{22}^{*}{}_{max} = \frac{2\beta}{5(\beta+2)} \tag{3.27}$$

A series of individual calculations, using the series (3.18) reveals that $\sigma_{11}^{*}{}_{max}$, $\sigma_{22}^{*}{}_{max}$ are given to within 5% error in the interval $.1 \leq \beta \leq 10$ by eq. (3.27).

4. Concluding Remarks

In the application of eq. (3.27) the following relationship gives the temperature difference causing failure (ΔT) in °C., if the tensile strength and Young's Modulus are in p.s.i. and coefficient of thermal expansion in $°C^{-1}$ and $\sigma^*_{max} = \frac{(1-\mu)St}{\alpha E \Delta T}$, then:

$$\Delta T = \frac{2.5\left(\frac{\beta}{3}+2\right)(1-\mu)}{\alpha E} St \qquad 4.1$$

where β = Biot's Modulus = rH

μ = Poisson's Ratio

E = Young's Modulus

α = Coefficient of Thermal Expansion

St = Breaking Tensile Stress

r = Radius and H = surface heat transfer coefficient

Equation 4.1 appearing above is valid for the heating and cooling of a sphere if (rH) is within the range of .1 to 10. Within this range the above equation is accurate within 5%. For ceramic materials heated or cooled in air or in a liquid salt the (rH) will undoubtedly fall within this range. However, there may be circumstances which require the use of an equation fitting the extremely large or extremely small values of $(rH)^*$. For that reason the asymptotic values appearing below have been determined.

Straight forward but lengthy calculations using the series (3.18) and a second expansion for (f) in terms of error functions, reveals that

*An equation which fits the cooling conditions much better for (rH) around 10 appears below:

$$\Delta T = \frac{(.525 + 1.5\beta)(1-\mu)St}{\beta \alpha E}$$

the asymptotic solutions for the maximum stress are:

for $\beta H \ll 1$

$$\sigma_{11\,max} = \frac{2\alpha E \beta}{1-\mu} \Delta T \quad \text{at } \xi = 0 \qquad 4.2$$

$$\sigma_{22\,max} = \frac{\alpha E \beta}{1-\mu} \Delta T \quad \text{at } \xi = 1 \qquad 4.3$$

for $\beta H \gg 1$

$$\sigma_{11\,max} = \frac{.385\,\alpha E}{1-\mu} \Delta T \quad \text{at } \xi = 0 \qquad 4.4$$

$$\sigma_{22\,max} = \frac{\alpha E \left(1 - \sqrt{\frac{\epsilon}{1+\beta}}\right)}{1-\mu} \Delta T \quad \text{at } \xi = 1 \qquad 4.5$$

Figure 1 is a plot of (σ^{*}_{max}) against (β) and indicates the manner in which the nondimensional stresses in the sphere vary with changing Biot's Modulus.

One of the advantages of an unsteady state test for thermal shock is that it enables one also to determine the time to maximum stress for a simple shape. The time to maximum stress, of course, may be used to determine the time at which failure will occur in the specimen after it is subjected to the single heat shock, provided the crack which indicates failure propagates to an extent where it may be consistently determined. The time to maximum stress (θ') is related to the radius of the sphere (r) and the thermal

diffusivity (α) by the relationship appearing below:

$$\theta' = \frac{f' r^2}{\alpha} \qquad 4.6^*$$

Nondimensional time (f) as a function of (β) is shown in Figure 2.

TESTING TECHNIQUES

A. Thermal Shock Tests

1. Specimens

The shape, size, and material of the specimen used for the thermal shock tests were the first experimental considerations. The solid sphere is a convenient shape for experimental use; however, forming procedures for this shape are not as simple as for some other shapes. The deciding factors in the selection of this shape were: first, very few assumptions were required to match experimental and theoretical boundary conditions and second, a good source was found for fabricating this shape.

A selection of the material to be used presented several problems. In order for the sphere to qualify as a homogeneous and isotropic material and still be considered an elastic substance it should ideally be a brittle substance of one single composition and continuous structure. In addition this substance should have no physico-chemical changes taking place within the range where it is still an elastic body (or at least over the temperature range selected for study.) The material selected was Coors' grinding ball material designated as type AB-2 ceramic - high strength alumina. Microscopic examination of the structure of this material indicated a very dense uniform cross section having a very high predominance of one phase - alumina. Although this material is not microscopically homogeneous it is macroscopically

*Much of the basic data for this equation and (4,1) were obtained from "Zeitschrift Des Vereines Deutscher Ingenieure" BD. 69, NR. 21 MAI 23, 1925, pa. 705-11.

homogeneous, i.e., volumes of the order of $1mm^3$ may be considered equivalent with respect to E, C, α, α, and S_t. Also Coors was able to form all specimens in the shapes required (for example, the cylinder for thermal diffusivity etc.). Five ball diameters were selected for study - 1, $1\frac{1}{4}$, $1\frac{1}{2}$, 2, and 3".

After receipt of the balls, outwardly imperfect ones were discarded. All remaining balls were measured for degree of roundness, and a check was made on water absorption (porosity), density and average diameter.

2. Testing

Tests were conducted on these balls using two thermal shock conditions; one, in a salt bath having a rather high surface heat transfer coefficient and two, in an air radiation boundary condition with a smaller surface heat transfer coefficient.

a. Liquid Boundary Condition - Heating

After the balls had reached uniform room temperature they were placed in a fine wire basket and immersed by hand into the salt bath* of a prearranged temperature. See Figure 3. The time required to fracture the ball was recorded. No difficulty was experienced in determining failure, as the balls exhibited complete fracture whenever a crack was started. (This fact was corroborated by immersing the ball in Zyglo penetrant† and examining under ultraviolet light to determine fine cracks. The ball was then fractured by impact and examined again for cracks.) If no failure occurred the ball was not tested again. At least ten balls were tested at each temperature. The temperature range where fracture occurred was studied and the (Δ T) values selected at a point where 50% of fracture occurred. See Figure 4. This plot indicates the percentage of one inch balls that

*Hitec - Manufactured by E. I. DuPont De Nemours & Company

†Zyglo - Manufactured by Magnaflux Corporation

fractured at each temperature interval. For this particular plot 500 balls were tested. (It may be seen that the plot approaches a normal distribution curve.) The time to maximum stress (θ') was obtained by: first, determining the 10°C cell centered upon the temperature corresponding to 50% failure of the ball and second, averaging the times to failure in this cell. The temperature difference causing failure and time to maximum stress were determined for the five sizes of balls, i.e., 1, $1\frac{1}{4}$, $1\frac{1}{2}$, 2 and 3".

b. Liquid Boundary Condition - Cooling

After the balls had reached uniform room temperature they were placed in the pipes of a gas fired furnace shown in Figure 5. Thermocouples were placed in the tubes adjacent to the escapement device and the gas adjusted to obtain a uniform temperature on all lower level balls. The temperature of the salt bath was then adjusted to obtain the proper temperature difference. At least 10 balls were dropped into the salt bath at each temperature difference. The temperature range where fracture occurred was studied and the ($\triangle$T) selected at a point where 50% of fracture occurred. This procedure was used to study the temperature difference causing fracture in the one and one quarter inch balls. The time to maximum stress could not be determined in these tests because the time was too short.

c. Air-Radiation Boundary Condition - Heating

The balls were prepared in the same manner for this test as for the salt bath heating. After the furnace had reached a prearranged temperature the hearth was lowered and the ball placed on the three-prong support on the hearth. See Figure 6. The hearth was raised immediately, plunging the ball into a uniformly heated chamber. The time required to fracture the ball was

recorded. Again no difficulty was experienced in determining failure as the balls exhibited complete fracture whenever a crack was started. Viewing ports were provided in the furnace to aid in the determination of fracture time. If no failure occurred the ball was not tested again. At least ten balls were tested at each temperature. The temperature range where fracture occurred was studied and the (Δ T) and (θ') values selected. The same procedure was carried out for several sizes of balls, i.e., $1\frac{1}{4}$, $1\frac{1}{2}$, 2 and 3".

d. Air-Radiation Boundary - Cooling

A number of balls were tested for the temperature difference causing failure upon cooling in air. The balls were placed on the same three prong support used for the heating experiment. The hearth was raised placing the ball in the heating chamber and the furnace temperature increased until the desired elevated temperature was reached. The ball was allowed to reach uniform temperature, then the hearth was lowered and the ball removed from the hot three prong support and placed on another similar support exposed to the room atmosphere. The approximate temperature difference causing failure was determined for a small number of balls. Because of the nature of the boundary condition of the cooling medium, i.e., a large volume of stagnant air at room temperature, it was difficult to clarify the very scattered results obtained. (Times to failure were recorded from several seconds out to nearly an hour, consequently no data have been reported).

B. Thermal Expansion

The thermal expansion equipment used in this study has been described by A. Lieberman.[1] The expansion of this material was measured on a 3/8" chip of a fractured ball both using the quartz and the sapphire dilation parts. With the sapphire parts, data were obtained up to 1400°C. A heating rate of

[1] A. Lieberman and W. B. Crandall, "Design and Construction of a Self-Calibrating Dilatometer for High Temperature Use", J.A. Ceramic Society 35 (11) 304-308 (1952).

3°C. per minute was obtained using a temperature program controller.

C. Thermal Diffusivity and Surface Heat Transfer Coefficient

An unsteady state method was used to measure thermal diffusivity and surface heat transfer coefficient of the Coors material. This method has been reported by H. S. Levine[2]. Semi-infinite cylinders, 1" diameter by 4" long, were formed having 1/8" holes along the cylindrical axis. At least three hole depths were required to insure accuracy in the measurements.

The method consists of plunging the semi-infinite cylinder with a thermocouple imbedded in the 1/8" hole, into a uniform heat bath, and taking temperature readings on the thermocouple as the specimen is heated or cooled. Figure 7 is a diagram of the apparatus used for air radiation boundary studies. The specimen was placed on the pedestal support with the thermocouple in place. The racking device was used to plunge the specimen into the radiation heat bath. A portable precision potentiometer was used to record the temperature rise as a function of time at that point within the specimen. The test was repeated for the same specimen at 440, 600, 800, 1000 and 1200°C then another specimen of exactly similar structure but different hole depth was placed on the pedestal and the same test run. This procedure was repeated for each of 4 hole depths. From the data obtained, thermal diffusivity, Biot's Modulus and Surface Heat Transfer Coefficient were calculated for these temperatures.

So that duplicate experiments could be run for both the thermal shock test and the surface heat transfer coefficient measurement, it was necessary to devise a method of moving a semi-infinite cylinder into the same heating or cooling condition as was used to fracture the balls. Consequently, double heating chambers were constructed. Figure 8 is a drawing of the apparatus used for heat transfer experiments employing two air

[2] H. S. Levine, "An Unsteady-State Method for Measuring Thermal Diffusivity at High Temperatures", Technical Report June 15, 1950, ONR Alfred, New York.

radiation media temperatures. The upper furnace was operated at a temperature above that of the lower one. It was not necessary to make these measurements with tungsten and molybdenum thermocouples in the lower temperature range where base metal couples would suffice. The top furnace in Figure 9 was operated at temperatures either above or below the temperature of the salt bath below it. Of course it is impossible to use exactly the same temperature difference which caused failure of the ball because it would also cause failure of the cylinder. However, a temperature difference as close to this as possible was used. The method of obtaining the thermal constant was the same for these set-ups as for air, described in the previous section.

D. Modulus of Elasticity

The apparatus shown in Figure 10 was used to measure Young's Modulus of elasticity by a sonic method. Specimens 4" long by 3/3" in diameter were used. These specimens were ground to shape from torsional specimens prepared at Coors. An audio oscillator and amplifier with matched speaker were used to drive the specimen at one end by a number 30 platinum wire supporting that end of the specimen at a position just off its nodal point. A variable reluctance pick-up connected to another piece of number 30 platinum wire picked up the vibration from the other end of the bar. The signal from the variable reluctance cartridge was sent through a preamplifier and amplified to an oscilloscope or vacuum tube voltmeter to serve as detectors. An audio frequency meter of the Wien bridge null detector type readable to the nearest 5 cycles was coupled to the high impedance line of the generator. This meter was used to measure the frequency put out by the audio oscillator. A very simple Globar furnace was used to heat the specimen. The resonant frequency of the specimen vibrating in flexure was followed on the "scope" or the voltmeter as the specimen was heated up to 1000°C. From these data

it was possible to calculate (E) Young's Modulus using relationships described by Pickett.[3]

E. Modulus of Rigidity

The modulus of rigidity (E_s) does not appear in the thermal shock relationships, however, Poisson's ratio, and modulus of elasticity do appear. The necessity of measuring the modulus of elasticity suggests that an indirect method be used to measure Poisson's ratio from the relationship:

$$\text{Poisson's ratio} = \mu = \frac{E}{2E_s} - 1 \qquad 5.$$

Modulus of rigidity measurements were obtained using the apparatus shown in Figure 11. Rectangular-ended specimens having a cylindrical center section were prepared by Coors for these tests. The gage section measured 9/16" in diameter and 1-3/4" long. The method used has been described by J. A. Stavrolakis.[4] Two sapphire mirrors were attached to the ends of the gage section by platinum bezels. An optical lever system was used to measure the difference in the amount of angular displacement of these mirrors as one end of the specimen was twisted, the other end being fixed. The modulus of rigidity was measured by this method over the temperature range of 20 - 1000°C.

F. Tensile Strength

Previous work done in the field of thermal shock has stressed the importance of reliable strength data and the knowledge of possible weak shear strengths existing in the test specimen.[5] As a result of this work,

[3] Pickett, G., "Equations for Computing Elastic Constants From Flexural and Torsional Resonant Frequencies of Vibration of Prisms and Cylinders", ASTM Proceedings pa. 846-59. Vol. 45, 1945.

[4] Stavrolakis, J. A., Norton, F. H., "Measurement of the Torsion Properties of Alumina and Zirconia at Elevated Temperatures", J. A. Cer. Soc. 33 (9) 263-268 (1950).

[5] Kingery, W.D., and Bowen, L.J., "Thermal Shock Resistance of Brittle Materials, I General Theory," Presented at the 99th Meeting of the Electrochemical Society April 11, 1951.

a study was made of the strength of the Coors material by two methods.

The first tests were conducted using conical-ended test specimens and grips shown in Figure 12. The test specimens were prepared at Coors. The gage section was 3/8" in diameter and 1-5/8" long. Graphite shims were used to cushion the test specimen against the high temperature steel grip. A hydraulic pulling device with furnace attached was used to measure the tensile strength of the specimen. The grips as well as the specimen were enclosed in the furnace. Measurements were made between 20-1000°C.

The second tests were conducted using rectangular-ended torsional specimens shown in Figure 11. At the same time as measurements were being made to determine the modulus of rigidity, the loading on the specimen was increased rapidly until fracture occurred. Measurements were made between 20 - 1200°C.

RESULTS

A. Thermal Expansion

The thermal expansion curve using the sapphire dilation parts is shown in Figure 13. The coefficients for the respective temperature ranges are shown in Table I.

TABLE I
Coefficient of Thermal Expansion

Temperature	Coefficient of Thermal Expansion ($\times 10^{-6}$/°C)
25 - 1000	8.0
25 - 200	6.1
200 - 400	7.1
400 - 600	7.9
600 - 800	8.7
800 - 1000	9.9
1000 - 1200	11.5
1200 - 1300	16.3
1300 - 1400	2.0

B. Thermal Diffusivity and Surface Heat Transfer Coefficient

The surface heat transfer coefficient, Biot's Modulus and thermal diffusivity for the Coors materials is shown in Table II.

TABLE II

Heat Conduction Data

SALT

Temperature	Surface Heat Transfer Coefficient	Thermal Diffusivity
200	.30 cm^{-1}	39 x 10^{-3} cm^2/sec.
350	.48 "	29 "
400	.55 "	28 "
500	.65 "	24 "

AIR

440	.08 cm^{-1}	23 x 10^{-3} cm^2/sec.
600	.13 "	19 "
800	.20 "	17 "
1000	.32 "	14 "
1200	.40 "	14 "

C. Modulus of Elasticity

The modulus of elasticity of the Coors material from room temperature to 1000°C is shown in Figure 14. Table III represents the elasticity values over the same temperature range.

TABLE III

Modulus of Elasticity

Temperature °C	Modulus of Elasticity x 10^6 psi
25	31.40
200	30.95
400	30.37
600	29.70
800	28.79
1000	27.10

D. Poisson's Ratio

Figure 15 represents the modulus of rigidity values obtained between room temperature and 1000°C. Using the modulus of elasticity values from Table III and equation 5, Poisson's ratioswere calculated from corresponding temperatures. Table IV shows the values obtained.

TABLE IV
Poisson's Ratio

Temperature °C	Poisson's Ratio (μ)
25	.27
200	.22
400	.17
600	.14
700	.15
800	.38

E. Tensile Strength

The tensile strengths of the Coors material measured by the torsional method are shown in Figure 16 and Table V.

TABLE V
Tensile Strength psi

Temperature °C	Torsional
25	19,600
200	19,600
400	17,500
600	16,500
800	13,400
1000	9,500
1100	7,400
1150	6,300
1200	5,200

These data are in good agreement with those found using the other type of experiment i.e., direct pulling and are quite a bit simpler to run.

Figure 17 is a photograph of a torsional specimen which is typical of the type of fracture obtained. The explanation for the type stress developed is given below:

If a rod, fixed at one end, is subjected to a torsion resulting in shear λ at the surface, this pure shear may be resolved into tensions $(+\sigma)$ and $(-\sigma)$ oriented along the surface of the rod, perpendicular to each other, and at 45° to the axis of the rod. The relation between λ and σ is

$$\lambda = \frac{1}{2}[\sigma - (-\sigma)] = \sigma$$

It follows from this, that if a helical fracture is characteristic of a rod when only pure torsion is applied, the fracture must have been due to the action of the resolved tension at 45° to the axis of the rod. See Figure 18 below:

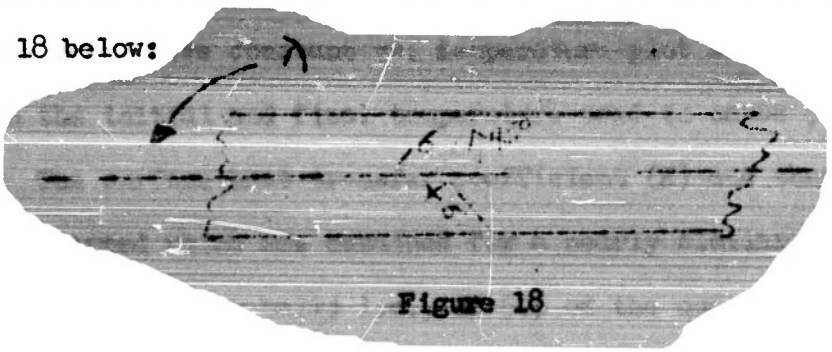

Figure 18

Therefore, even though the specimen was tested in torsion which would allow for shear releases to occur, none were found - all were helical tensile fractures. Thus, it was assumed that this material was predominately weak in tension and that failures should occur in tension at the center upon heating the sphere and in tension at the surface upon cooling. Further proof that this is true is obtained from an examination of the type of fracture obtained in the balls when heated. See Figure 19. In all cases, the fracture was radial from the center leaving a number of rosette fragments, indicating a tensile fracture initiated at the center.

F. Thermal Shock, Comparison of Experimental and Calculated Values -

An attempt has been made to compare experimental thermal shock values, (ΔT's) with the theoretically calculated values obtained using a fairly wide range of ($\mathcal{E}$). The experimental values were obtained from room temperature to 1400°C. The calculated values were obtained by substituting into the correct formula for the ($\mathcal{E}$) range covered by the experiment. The substitutional values were obtained by consulting the proper constant vs. temperature plot and introducing the values which applied. It has been assumed that a value should be substituted for the modulus of elasticity (E) and Poisson's ratio (μ) which corresponds to a mean temperature, i.e., a value from the respective constant vs. temperature plot at a temperature midway between the initial and final temperature used to cause 50% fracture of the balls. The surface heat transfer coefficient (H) and thermal diffusivity (α) was substituted which was obtained for a nearly similar experiment which had caused failure of the ball; i.e., if 50% of the one inch balls failed upon heating with a starting temperature of 25°C and a final temperature of 722°C, then the (H) and (α) values were found by the unsteady state method for the temperature difference having one half the final temperature of 722°C and the same starting temperature. The coefficient of expansion (α) was obtained from the slope of the straight line joining the expansion values for the starting and final temperature. The tensile strength (S_t) was obtained using the time to maximum stress to determine the temperature and thus the strength that must have been exceeded to cause failure.

It is evident that the above described procedure for introducing the proper "constants" into the thermal shock relationships is open to question. It seems quite evident that one should take some value for substitution which is intermediate between starting and final temperatures.

However, the exact position of this value can only be assumed. The half temperature values are probably as realistic as any that might be substituted for σ and E. The reason for selecting the temperature and thus the time for the strength data from the time to maximum stress values may not be obvious. Failure or fracture of the ball upon heating is known to take place by initiating a tensile fracture at the center. The temperature of the area where failure occurs may be closely estimated in the ball by taking the temperature from the "heating curves" of the semi-infinite cylinder for the time where failure occurred in the ball (of the same size). Then using this temperature, the strength may be obtained from strength versus temperature curve. Upon cooling the time to maximum stress is very short thus the temperature selected to use is that of the surface film. The temperature of this film would be near that of the final medium. In both the case of heating and cooling, one must consider more than just the area of the surface or center, for nearly all parts of the body contribute to the strength. Therefore, a value was substituted which was intermediate between this one and the mean.

Following the system set forth above, the (Δ T's) and (Δ T) were calculated for heating and cooling conditions in salt and heating in air. The calculated (Δ T) values may be compared with the experimental values by referring to Table VI.

TABLE VI

Experimental and Calculated Thermal Shock Values

	1	1¼	1½	2	3
Heating in Salt (Calculated)	736	648	559	448	352
Heating in Salt (Experimental)	722	600	575	540	500
Heating in Air (Calculated)	X	1442	1400	1135	1032
Heating in Air (Experimental)	X	1344	1228	1117	950

TABLE VI (Cont.)

Experimental and Calculated Thermal Shock Values

	1	1¼	1½	2	3
Cooling in Salt (Calculated)	736	648	559	448	352
Cooling in Salt (Experimental)	250	230	X	X	X

Time to maximum stress (t') values were calculated for each condition that could be checked experimentally. These values also may be compared with the experimental values by referring to Table VII.

TABLE VII

Experimental and Calculated Time to Maximum Stress Values

	1	1¼	1½	2	3
Heating in Salt (Calculated)	9	13	18	29	53
Heating in Salt (Experimental)	5	12	17	20	95
Heating in Air (Calculated)	X	27	36	60	107
Heating in Air (Experimental)	X	40	77	112	250

DISCUSSION OF RESULTS

A comparison of experimental and calculated (ΔT's) and (S_{max}) shows only fair agreement in light of all tests conducted. However, it should be emphasized here that this investigation has endeavored to go further than just to compare order of magnitudes, but has calculated numerical values for comparison with experimental tests.

It would appear that the experimental heating values in salt were too high compared with the calculated values and too low in light of calculated values for the cooling cycle. This situation would suggest that perhaps the balls were received with some nonuniform stress along their cross-section. If the surface of the ball was under tension and the center in compression as received, when the ball was heated to cause fracture, the thermo-stress developed would first have to reduce the compression in the

center before starting to develop the required tension to cause fracture. This would result in an overall larger stress and thus a greater temperature difference to cause failure. The same initial stress would cause the cooling temperature difference to be too small. To determine if this were a possible cause for the conflict between experimental and calculated values a number of balls were placed in crucibles and heated slowly to 1500°C and held for 8 hours. These balls were cooled slowly to relieve any stress which might have been present. Then a number of these balls were tested to determine their (Δ T). There was very little, if any, difference in the resulting (Δ T) from this experiment over the original value. From this test it was concluded that there were no initial stresses present in the balls.

One may look to all of the "constants" substituted in the thermal shock relationship and question the procedure used in their selection. However, the largest question undoubtedly may be raised regarding the strength and heat conduction values. Strength in particular is a most illusive property to determine. Two methods were used to determine strength involving two sizes and techniques. The direct pulling experiment is an indication of entire cross-section strength whereas the torsional experiment probably indicates the strength more as a surface property. The transverse rupture test might be a better indication of the proper strength here, however, it does not indicate possible weak shear strength. The size factor should not be over-looked also. The size of the thermal shock ball is larger than the gage section of either of the test specimens used to determine strength. It is possible that the size relationship here is in poor agreement. Also, the surface in contact with the test specimen may influence the strength value obtained. All strength measurements were made with air as the surface contact medium. Perhaps the strength of the specimen in contact with the salt

(especially on the cooling cycle where surface is so important) is strongly influenced by the surface contact of salt.

The surface heat transfer coefficient and Biot's modulus are most difficult to measure. The manner in which the experiment is run may strongly influence the values obtained. Therefore, it is important that as nearly similar conditions as possible be used for both the heat shock test and the experiment which derives the values used for (H) and ($\mathcal{E}$). It is difficult to establish the proper boundary condition for an experiment such as the one run in a salt bath. The nature of the heat transfer from the salt to the ball involving surface films etc., complicates the measurement of the surface heat transfer coefficient. The size of the specimen has an equal effect on the size of (,) as does the heat transfer coefficient. It is possible to change the size of the specimen and thus change the values of Biot's modulus by many times even for the same temperature difference. The way in which the size of the ball changes the temperature difference causing failure is shown in Figure 20. As the size of the ball is decreased the temperature difference causing failure increases rapidly. Accordingly it follows that if the size is decreased sufficiently the (ΔT) will become so large that it is impossible to cause failure of the ball under practical conditions. This is the situation found using the one inch ball in the air radiation medium. Actually, the condition of plastic flow is reached with this small ball which releases the stress, before failure can occur. In other words, the body is no longer elastic.

SUMMARY

A method has been developed for studying the thermal shock characteristics of a brittle substance. The method consists of a single cycle test of unsteady state nature. Two testing conditions have been selected - one having a rather high surface heat transfer coefficient in a liquid bath and the other having a small finite surface heat transfer coefficient in an air bath. These two conditions are at either extremes regarding the thermal shock usually given a substance in practice.

The only fair agreement found in the calculated and experimental data indicates that further investigation is necessary. The importance of certain factors, such as time to maximum stress, which was found to be in rather good agreement for the salt bath heat transfer cannot be over-looked. There are many applications in the high temperature - high stress field in which the concept of time to maximum stress might well be examined. For example, in the case where repeated high temperature heatings are made on a refractory piece, the cycling might be arranged so that the time to maximum stress was never reached for the particular heating cycle - although the (Δ T) was higher than that necessary to cause failure. Much is to be learned from this type of study which may be applied to actual situations. It must be emphasized, however, that this work has been conducted on one single set of conditions and the factors found here do not necessarily carry over into other situations.

ACKNOWLEDGEMENTS

The authors are indebted to Messers: Levine, Swarts, Bassett, Forry, Kinsman, Riker, Ridgeway, Hanna and Swanson for their aid in much of the experimental and theoretical work.

This work was carried out under contract N6-ori-143 between Alfred University and the Office of Naval Research.

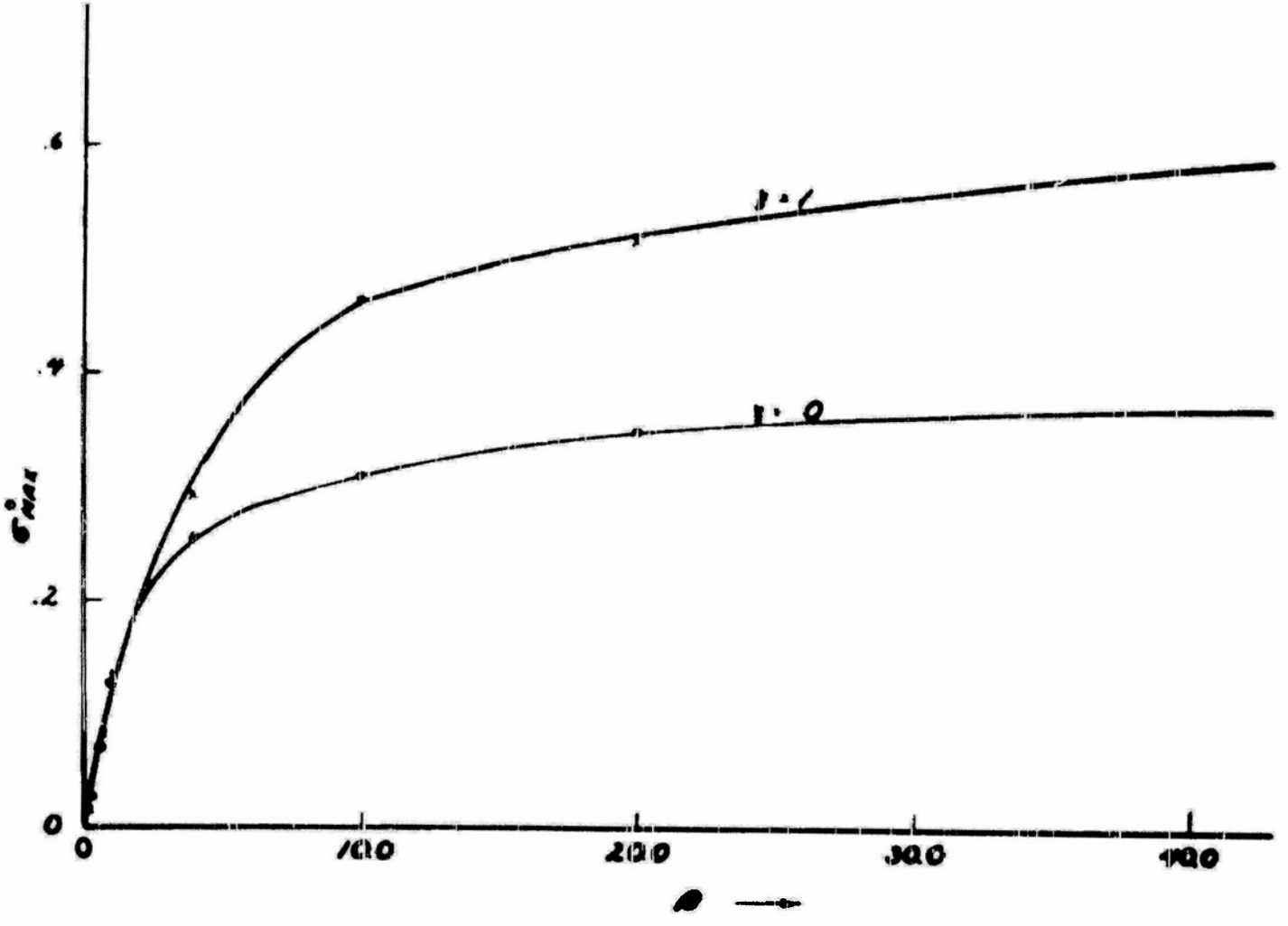

FIG. 1 SURFACE AND CENTER NON-DIMENSIONAL MAXIMUM STRESS VERSUS HEAT TRANSFER FOR A SPHERE.

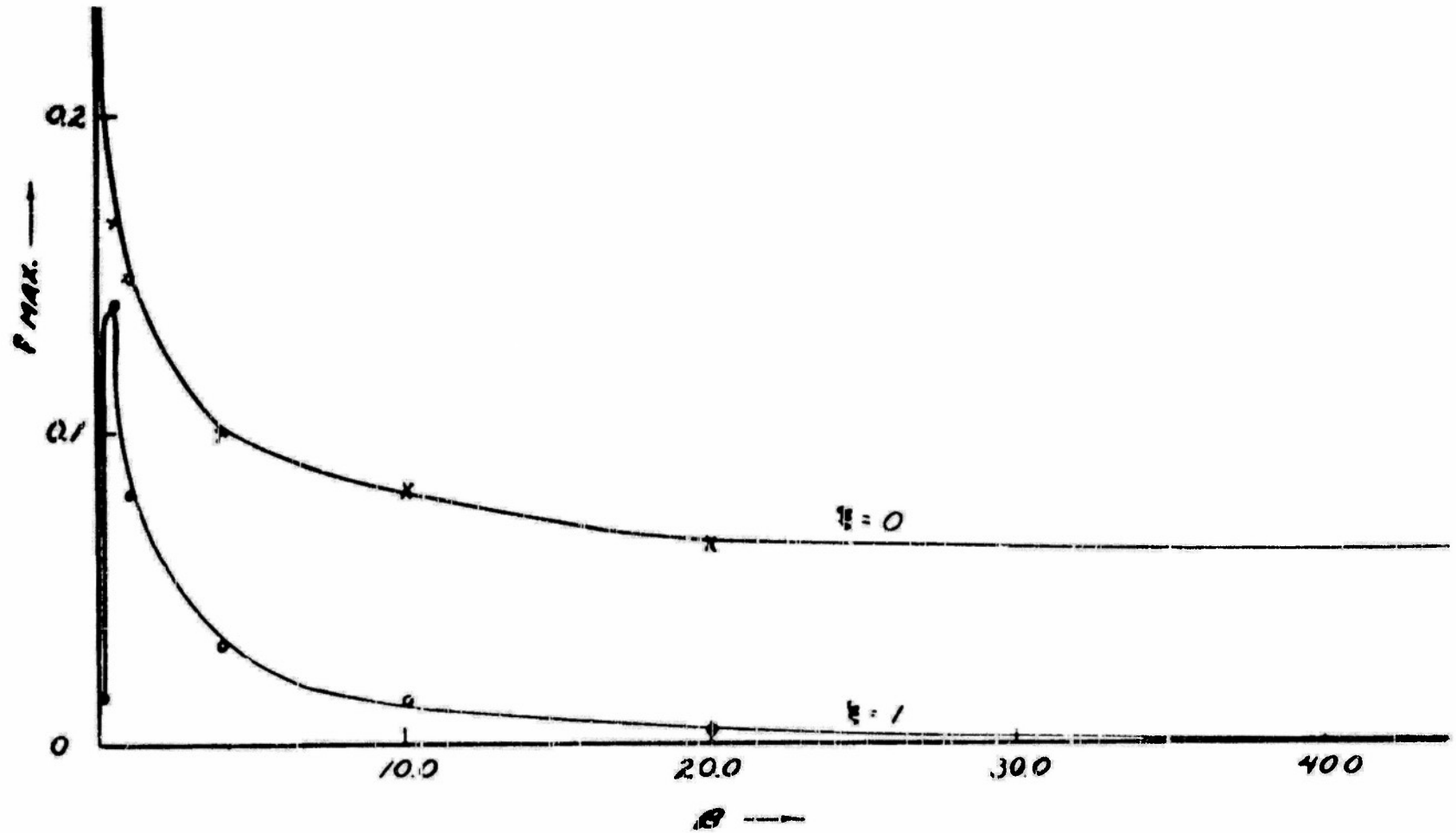

FIG. 2 CENTER AND SURFACE NON-DIMENSIONAL TIME VERSUS HEAT TRANSFER FOR A SPHERE.

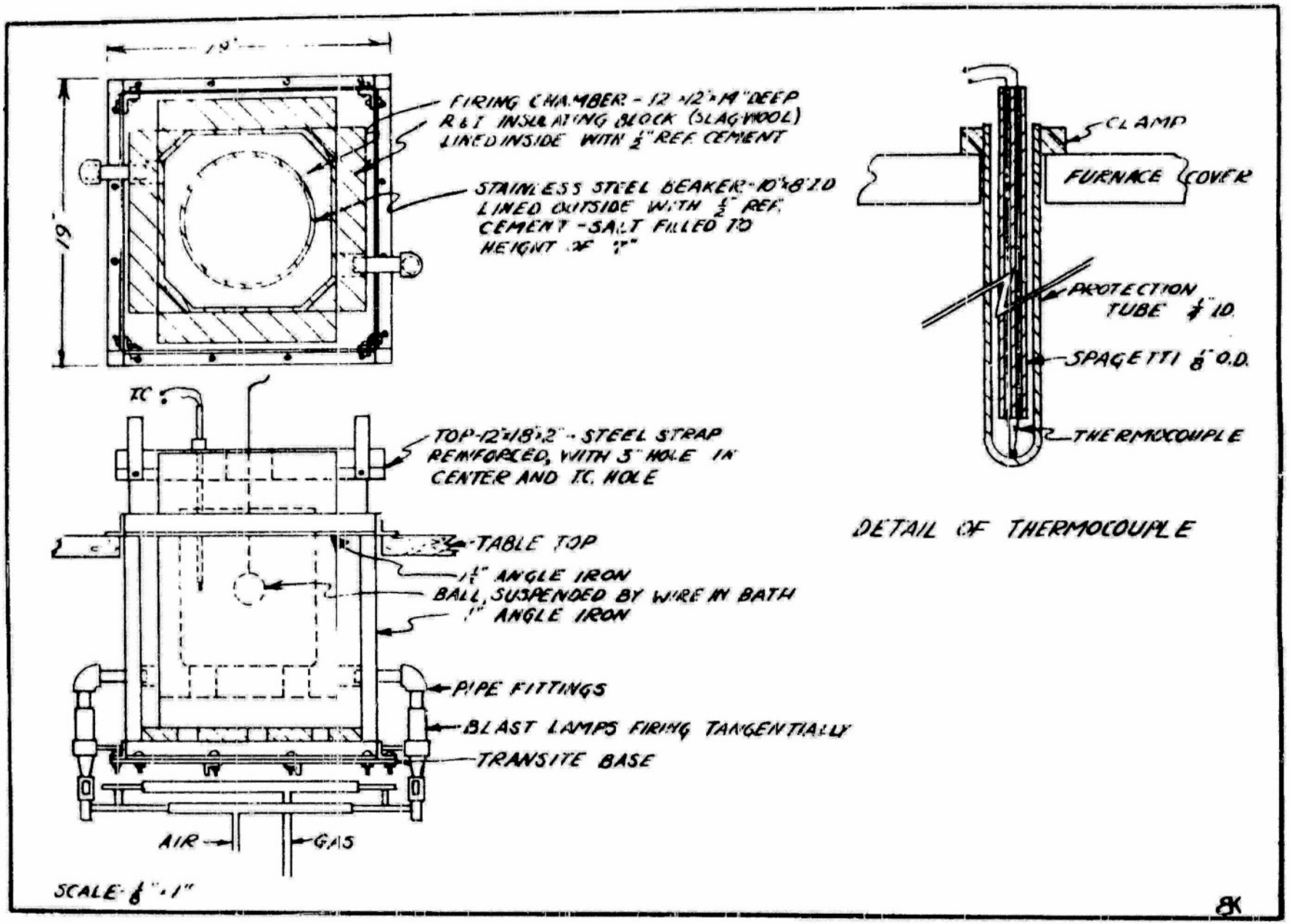

FIG. 3 MOLTEN SALT FURNACE.

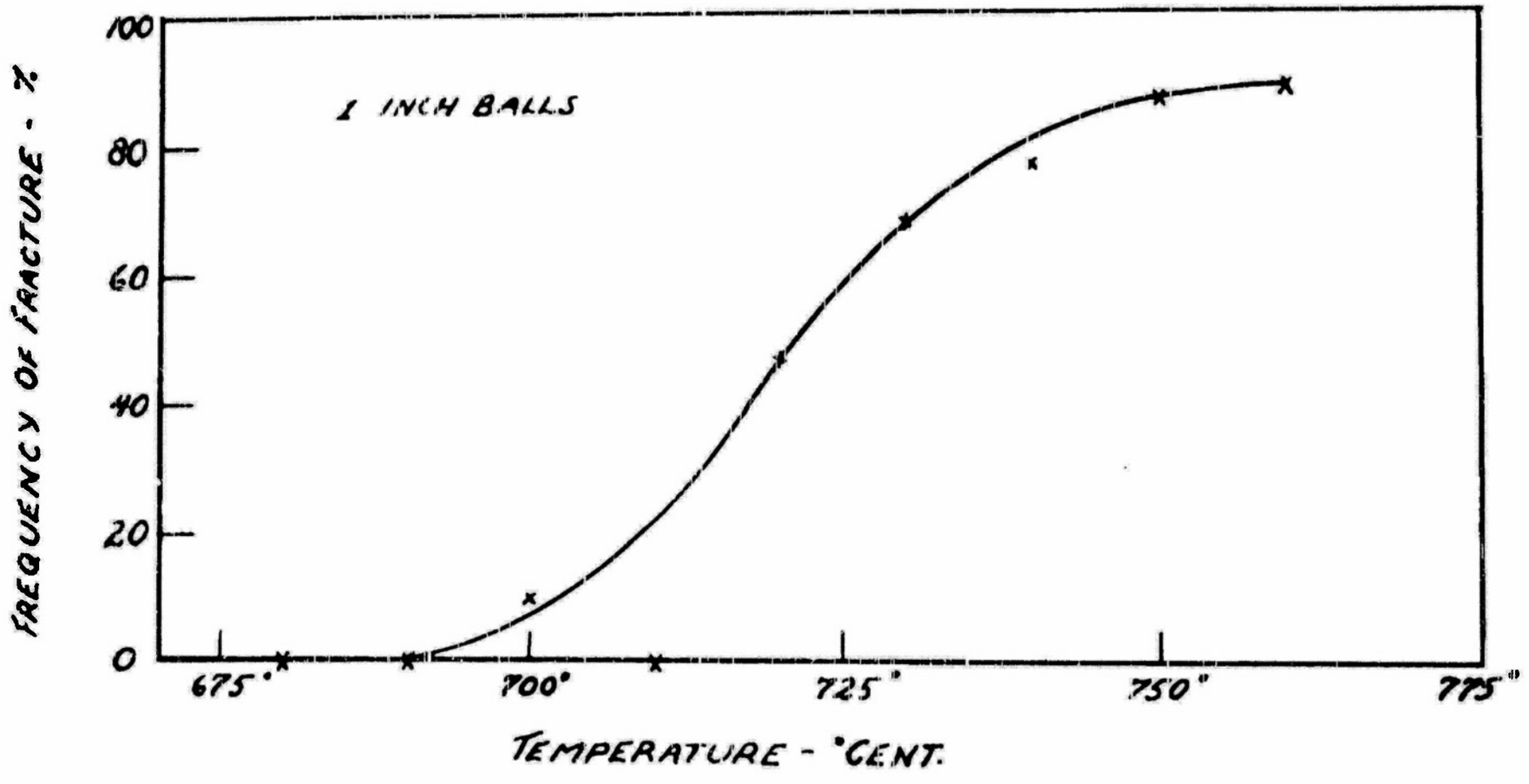

FIG. 4 PERCENT OF ONE INCH BALLS FRACTURING UPON HEATING IN SALT VERSUS TEMPERATURE.

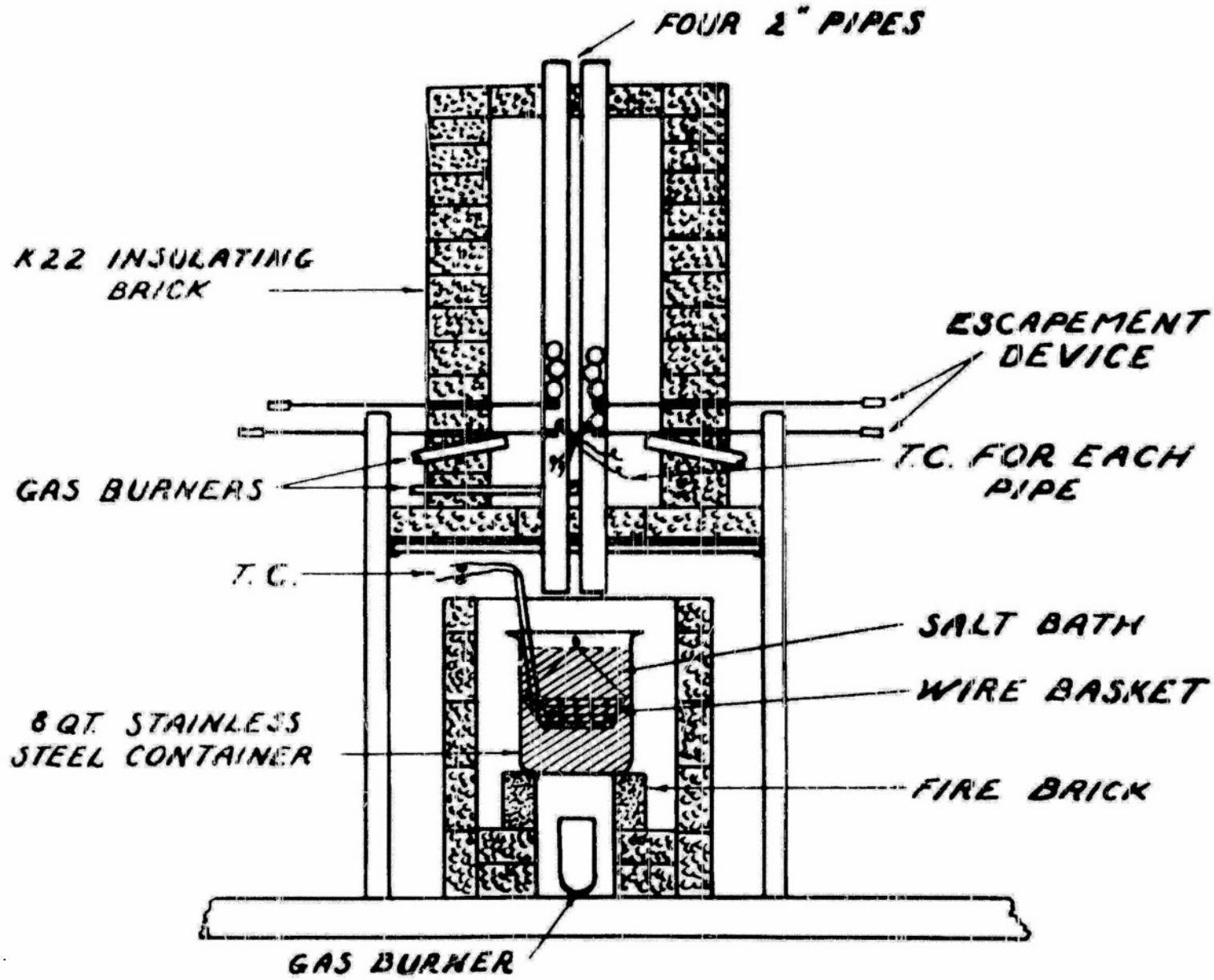

FIG. 5 THERMAL SHOCK FURNACE --- AIR TO SALT.

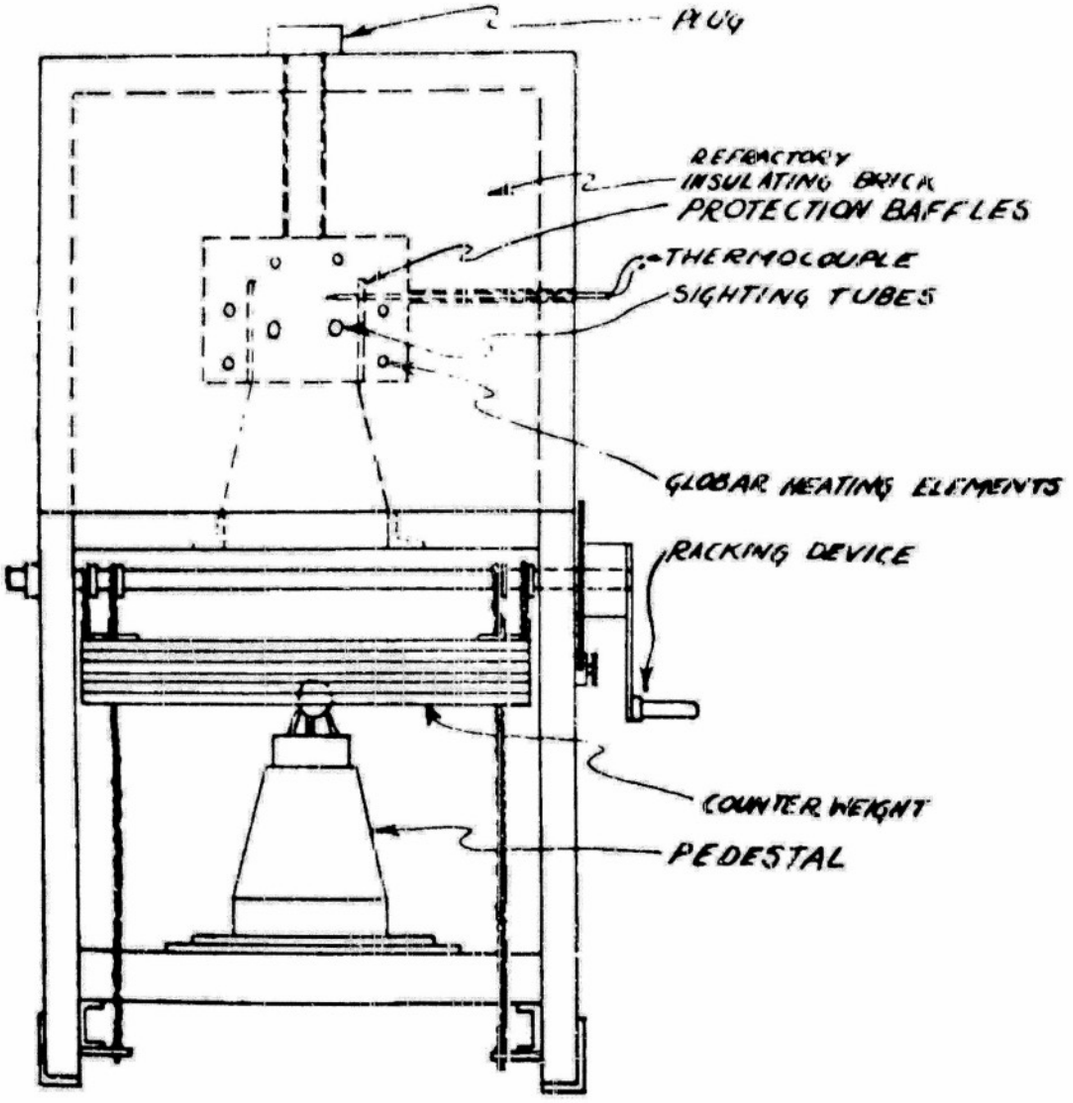

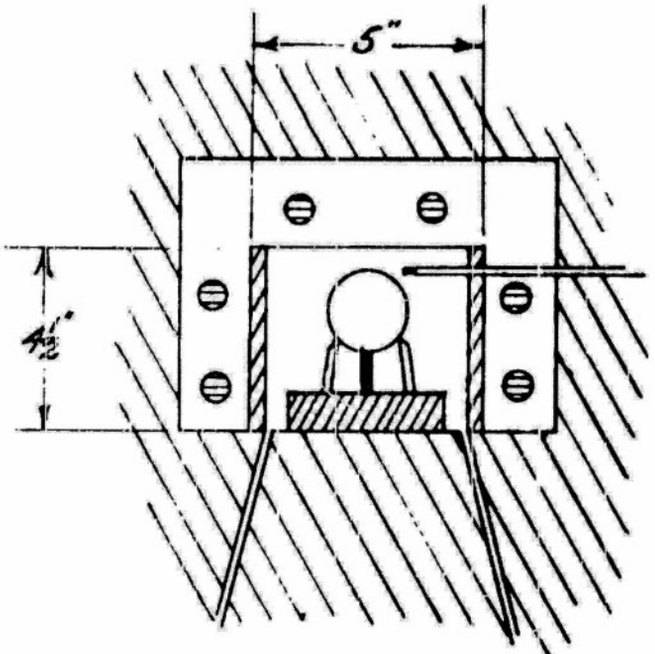

HEATING CHAMBER
SHOWING PEDESTAL AND SPECIMEN IN PLACE

FIG. 6 THERMAL SHOCK FURNACE --- AIR RADIATION.

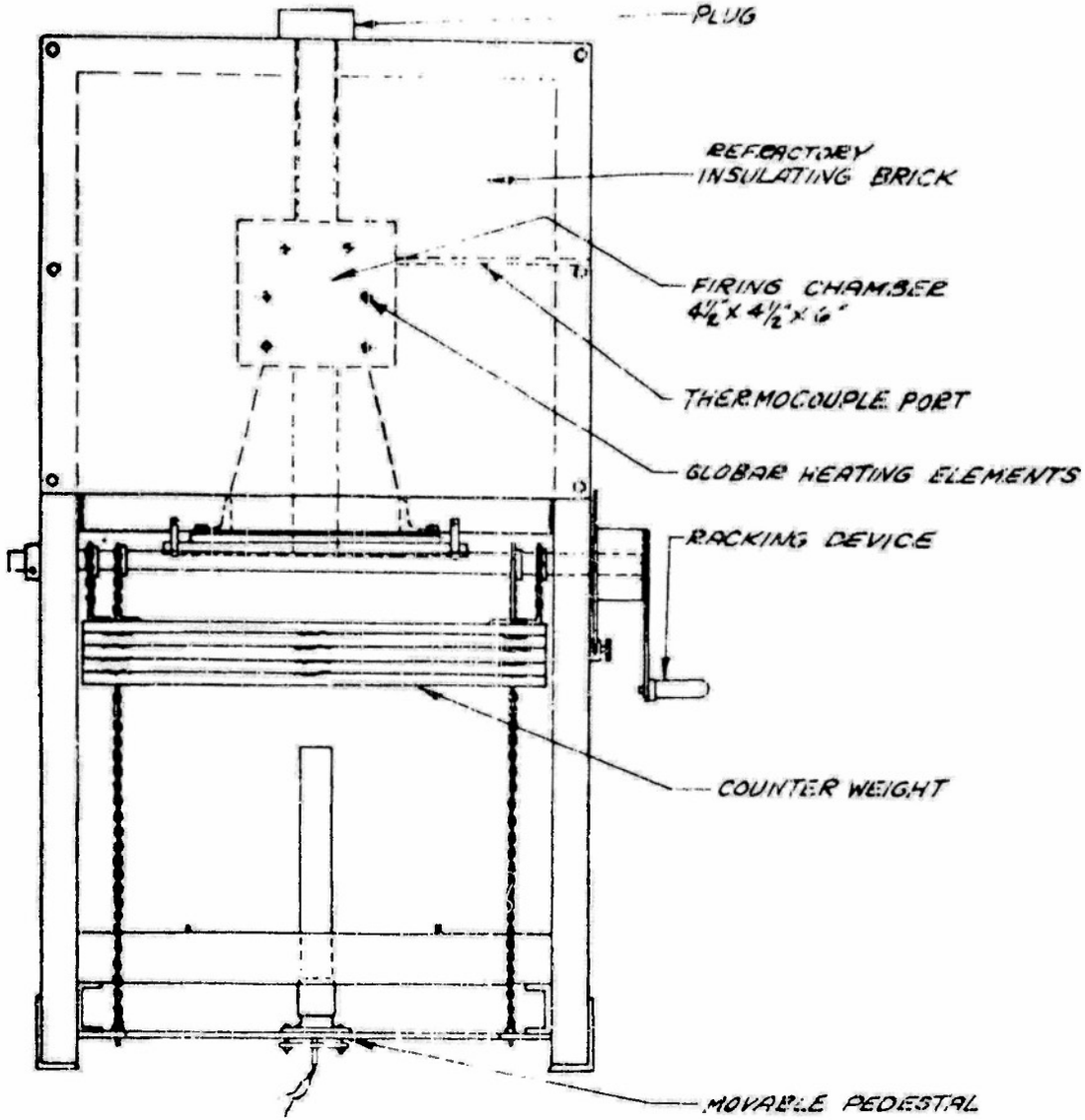

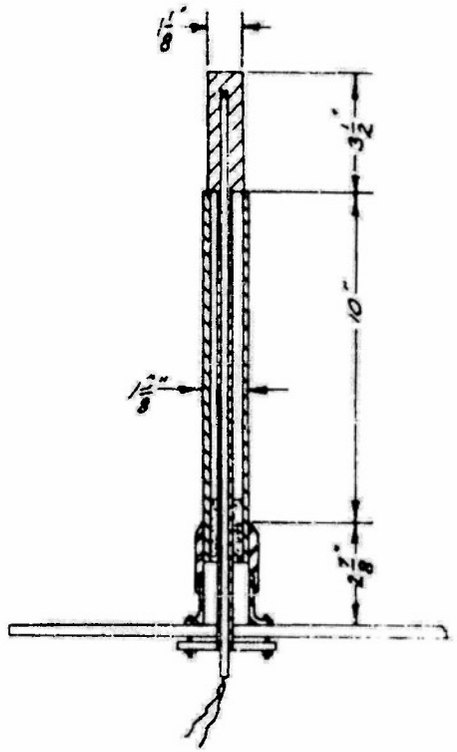

MOVABLE PEDESTAL
(WITH SPECIMEN MOUNTED)

FIG. 7 HEAT TRANSFER APPARATUS --- AIR RADIATION USING ONE FURNACE.

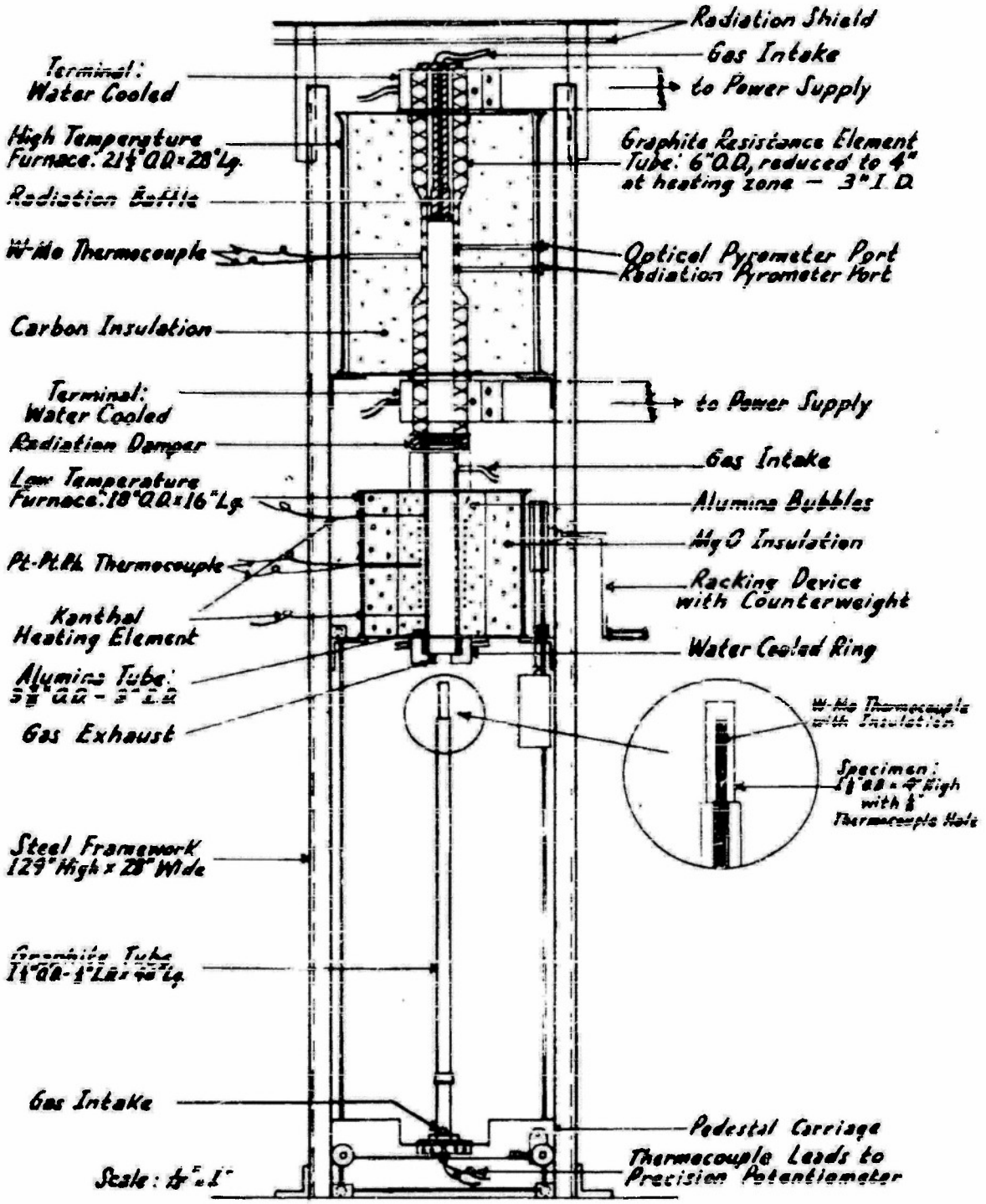

FIG. 8 HEAT TRANSFER APPARATUS --- AIR RADIATION USING TWO FURNACES.

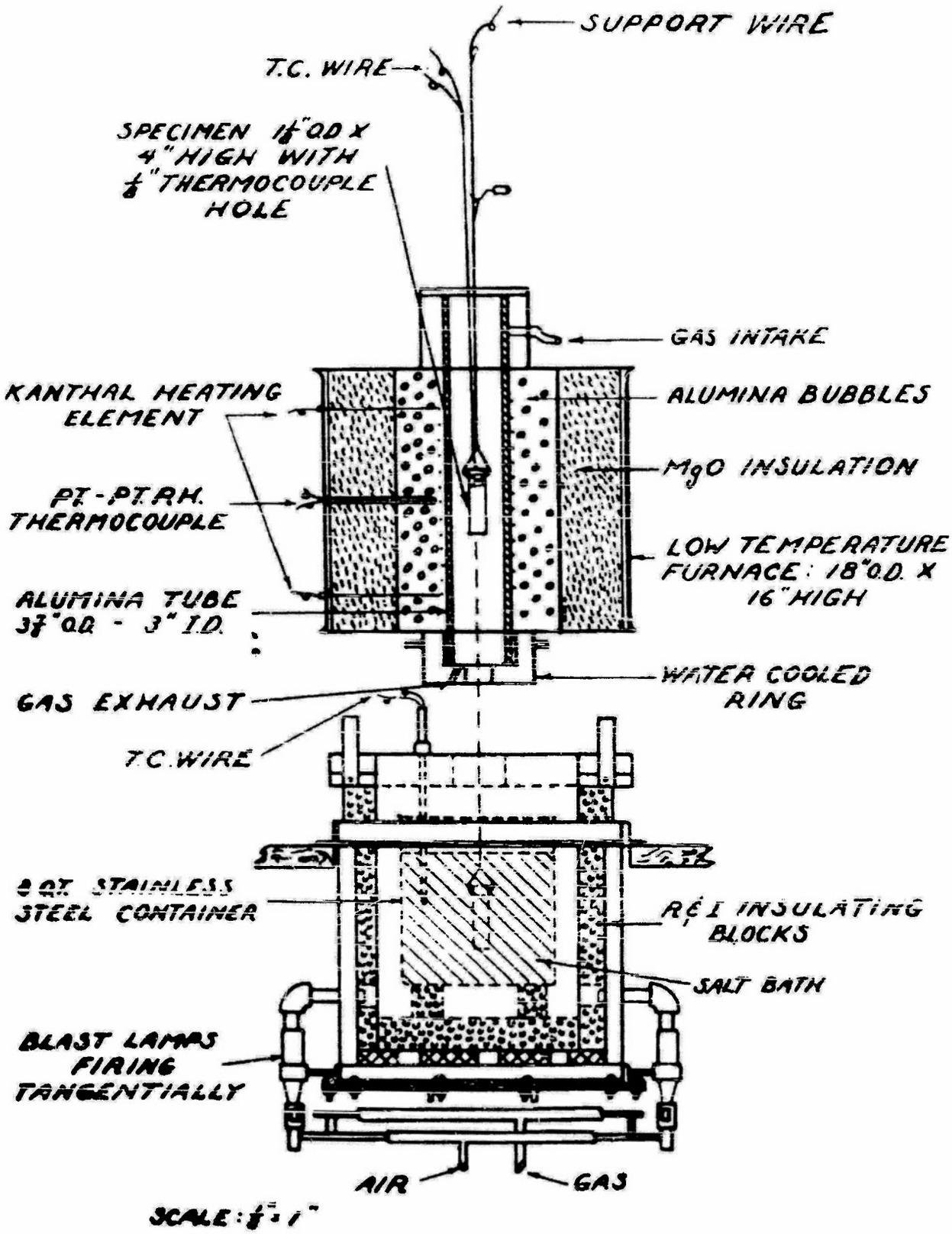

FIG. 9 HEAT TRANSFER APPARATUS --- AIR TO SALT.

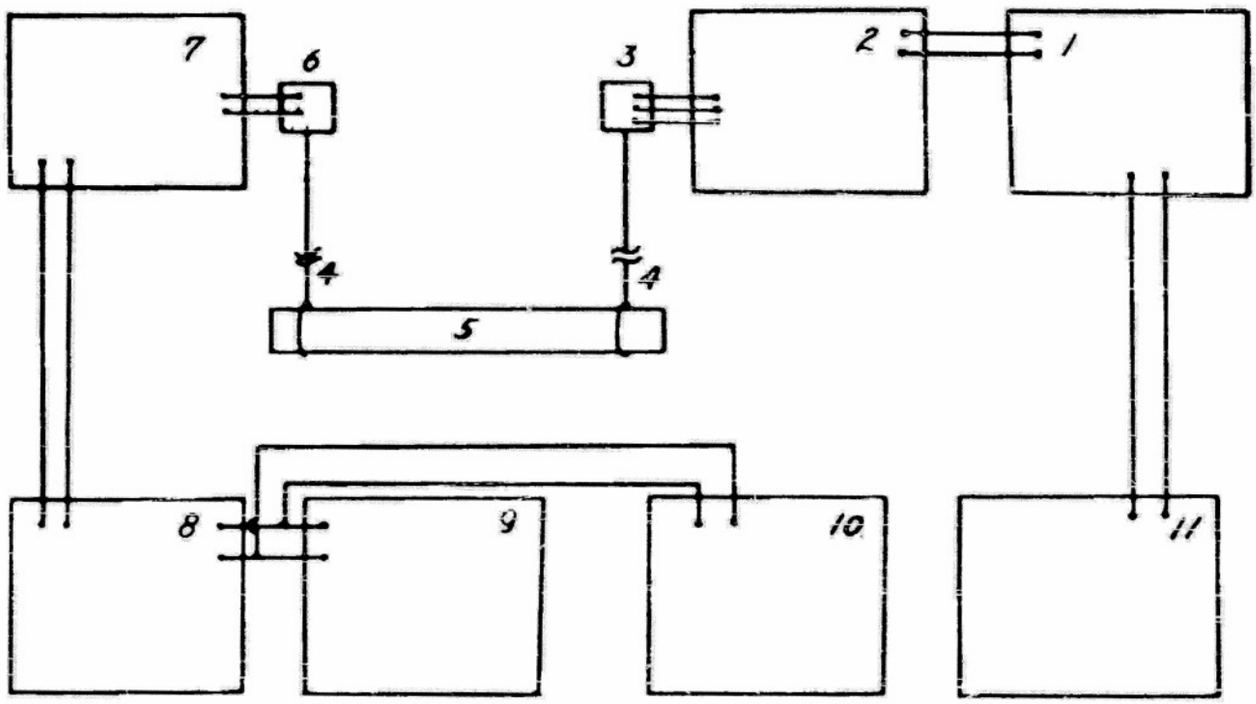

1 GENERAL RADIO TYPE 1302 - AUDIO OSCILLATOR WITH 600 & 5000 OHM OUTPUT IMPEDANCES TO 2 & 11 RESPECTIVELY.
2 AUDIO AMPLIFIER
3 ELECTRO - DYNAMIC TYPE SPEAKER WITH 0.4 OHM VOICE COIL
4 GAGE - 30 PLATINUM SUPPORT WIRES, EA. ABOUT 10 INCHES LONG.
5 SPECIMEN (CYLINDER)
6 PICKUP, A GENERAL ELECTRIC VARIABLE RELUCTANCE PHONOGRAPH CARTRIDGE WITH SHIELDED CABLE TO 7
7 HEATHKIT PREAMPLIFER - MODEL WA - P1.
8 HEATHKIT 20 WATT AMPLIFER, MODEL A-5
9 CATHODE RAY OSCILLOSCOPE
10 VACUUM TUBE VOLTMETER
11 GENERAL RADIO AUDIO FREQUENCY METER TYPE 1141 - A

FIG. 10 SONIC MODULUS OF ELASTICITY APPARATUS.

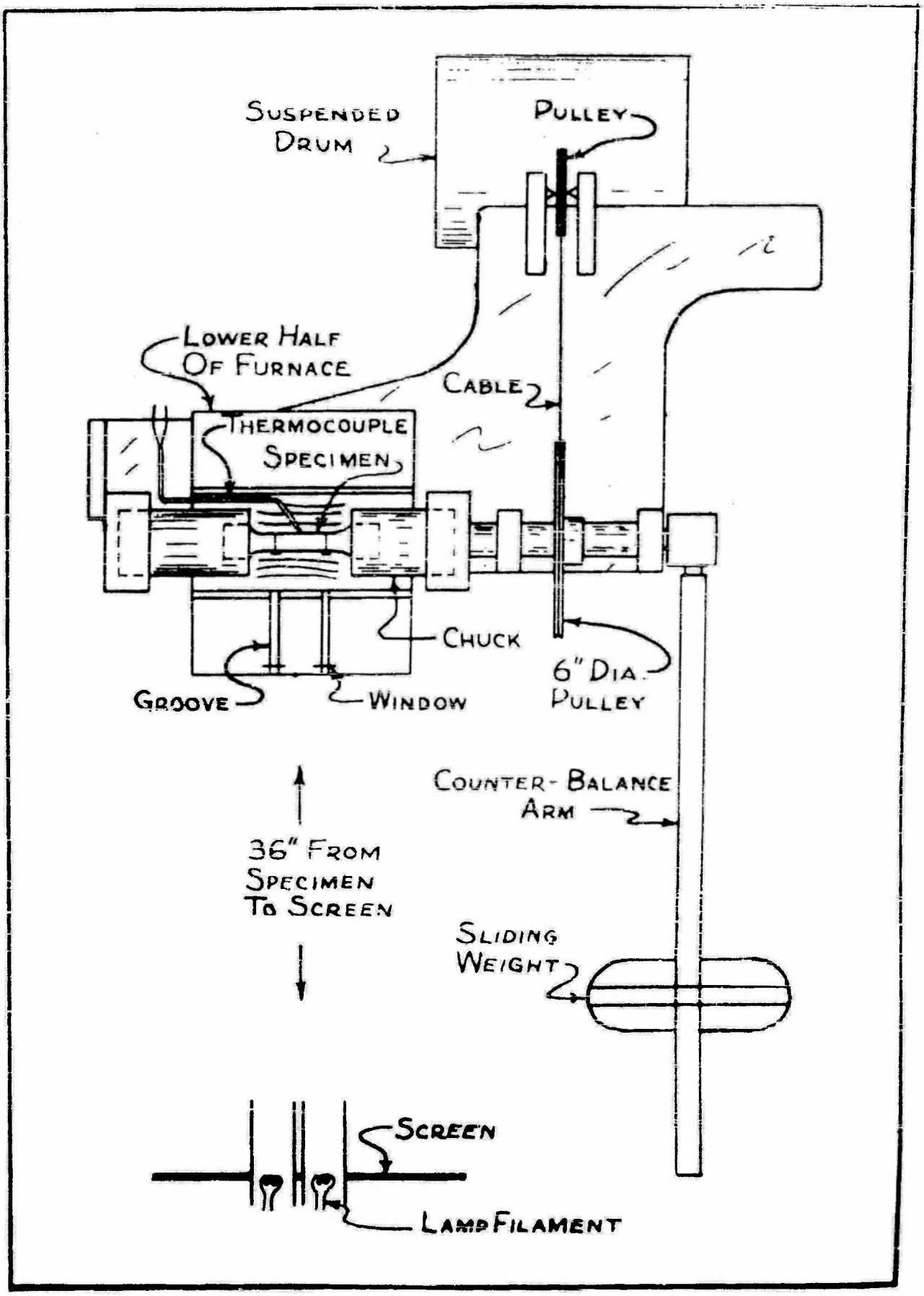

FIG. 11 TORSIONAL APPARATUS.

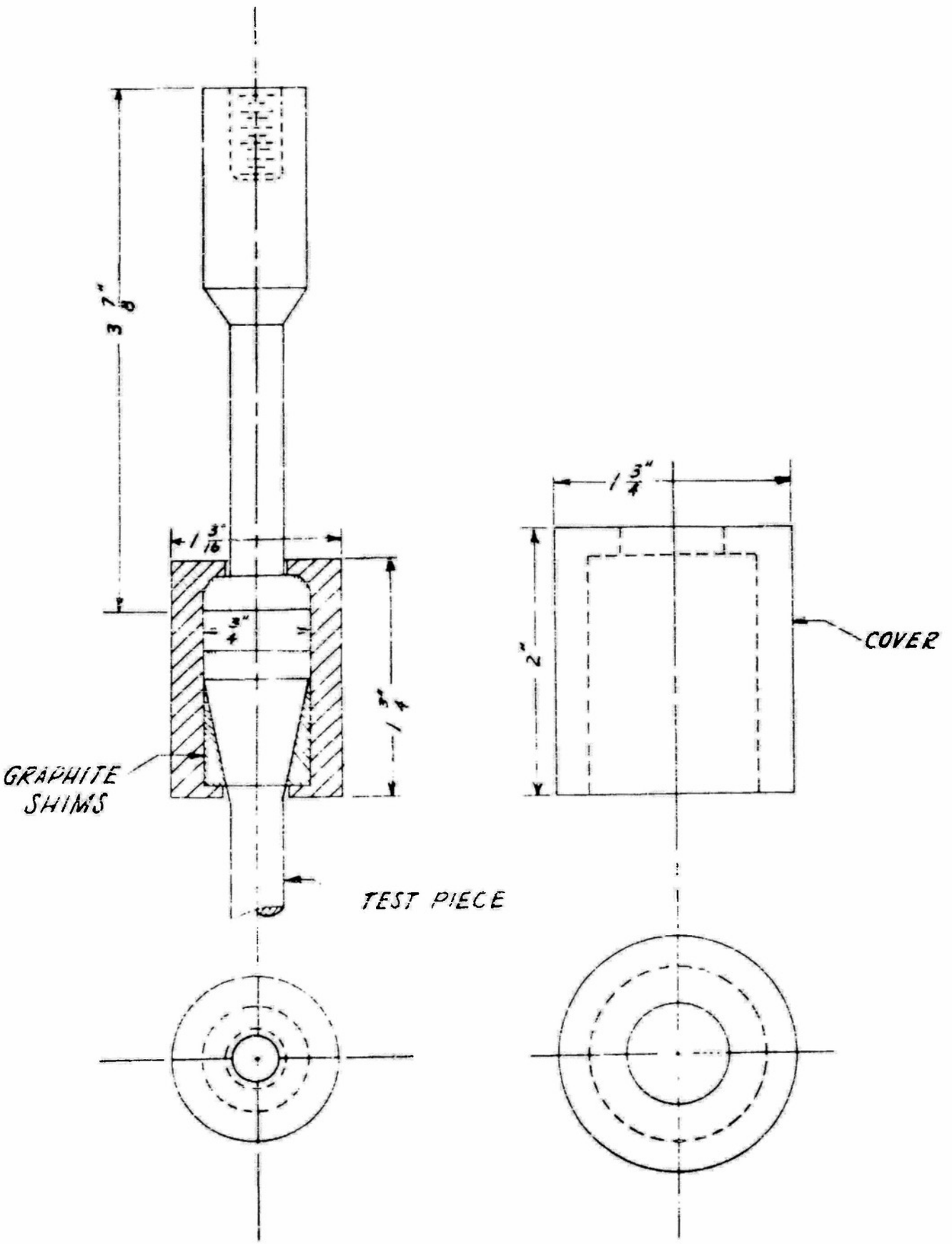

FIG. 12 TENSILE GRIPPING ASSEMBLY.

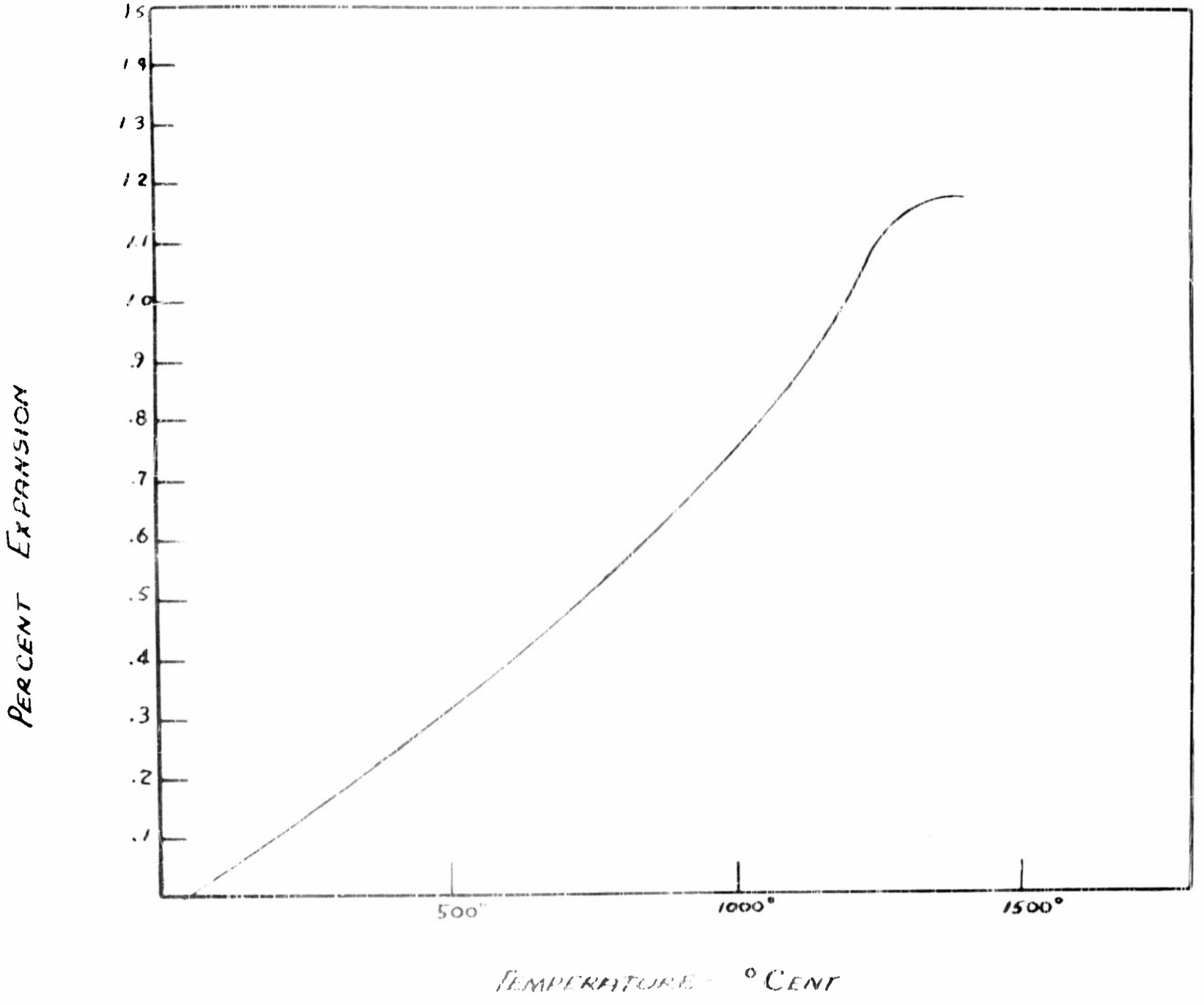

FIG. 13 THERMAL EXPANSION CURVE.

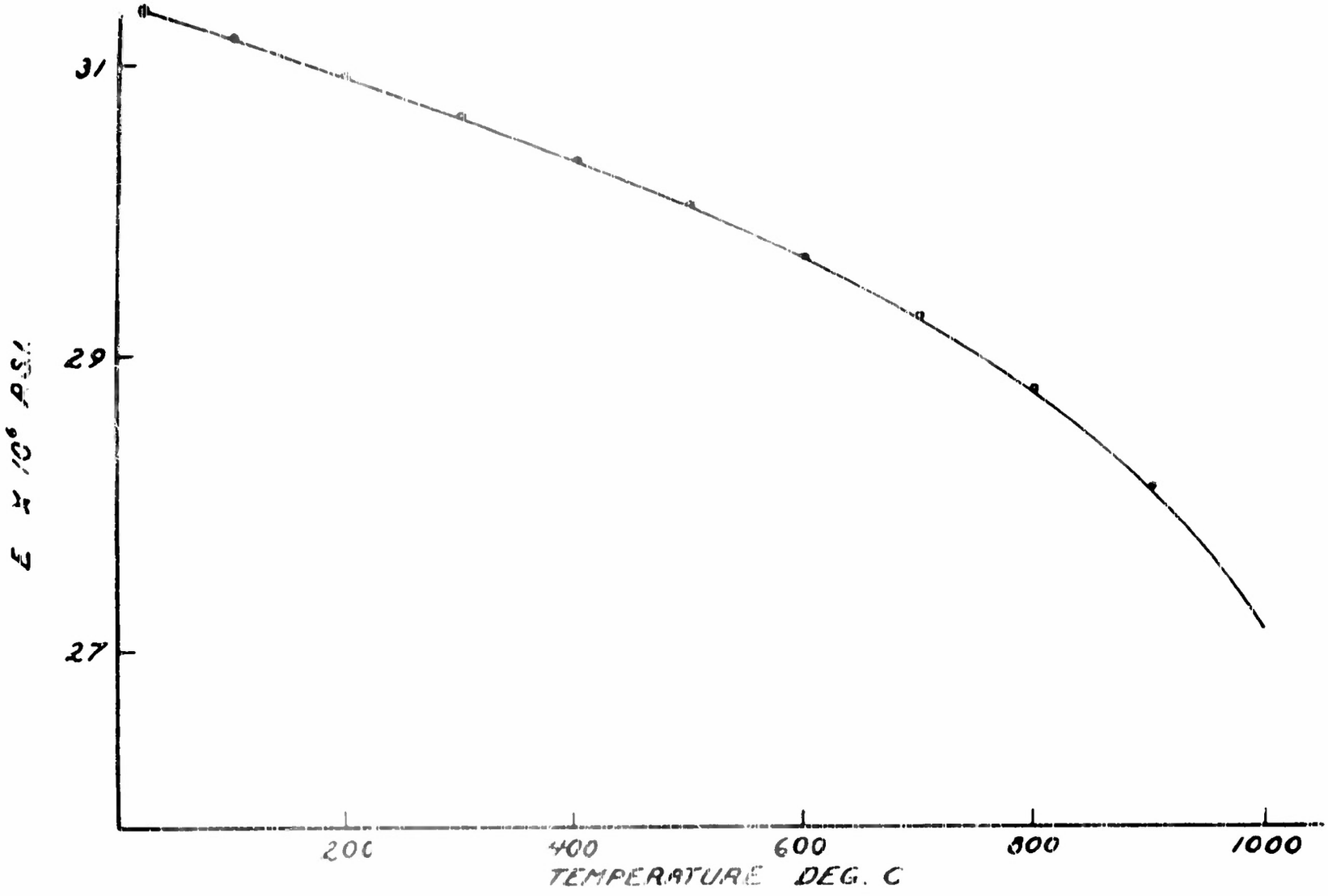

FIG. 14 MODULUS OF ELASTICITY CURVE.

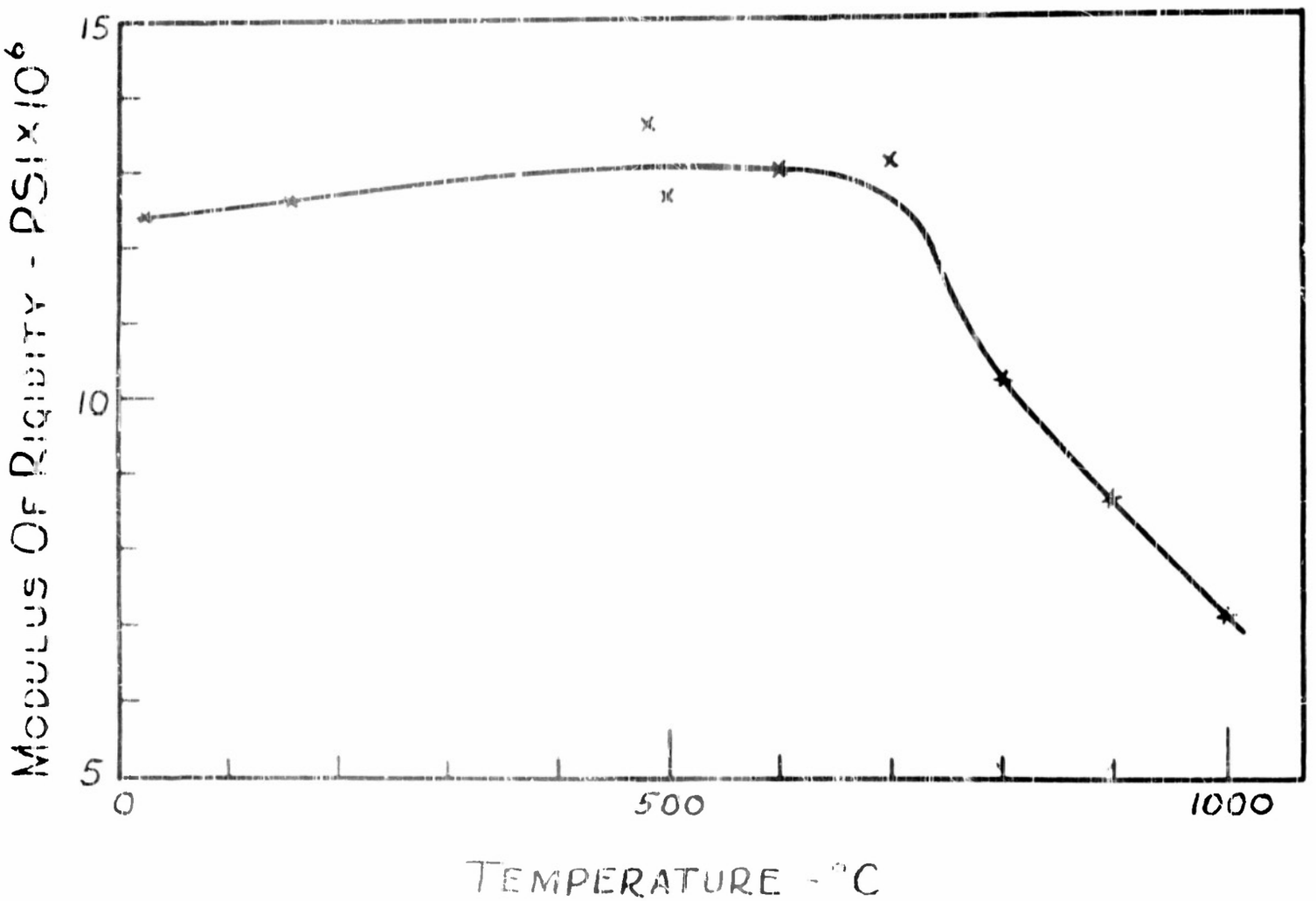

FIG. 15 MODULUS OF RIGIDITY CURVE.

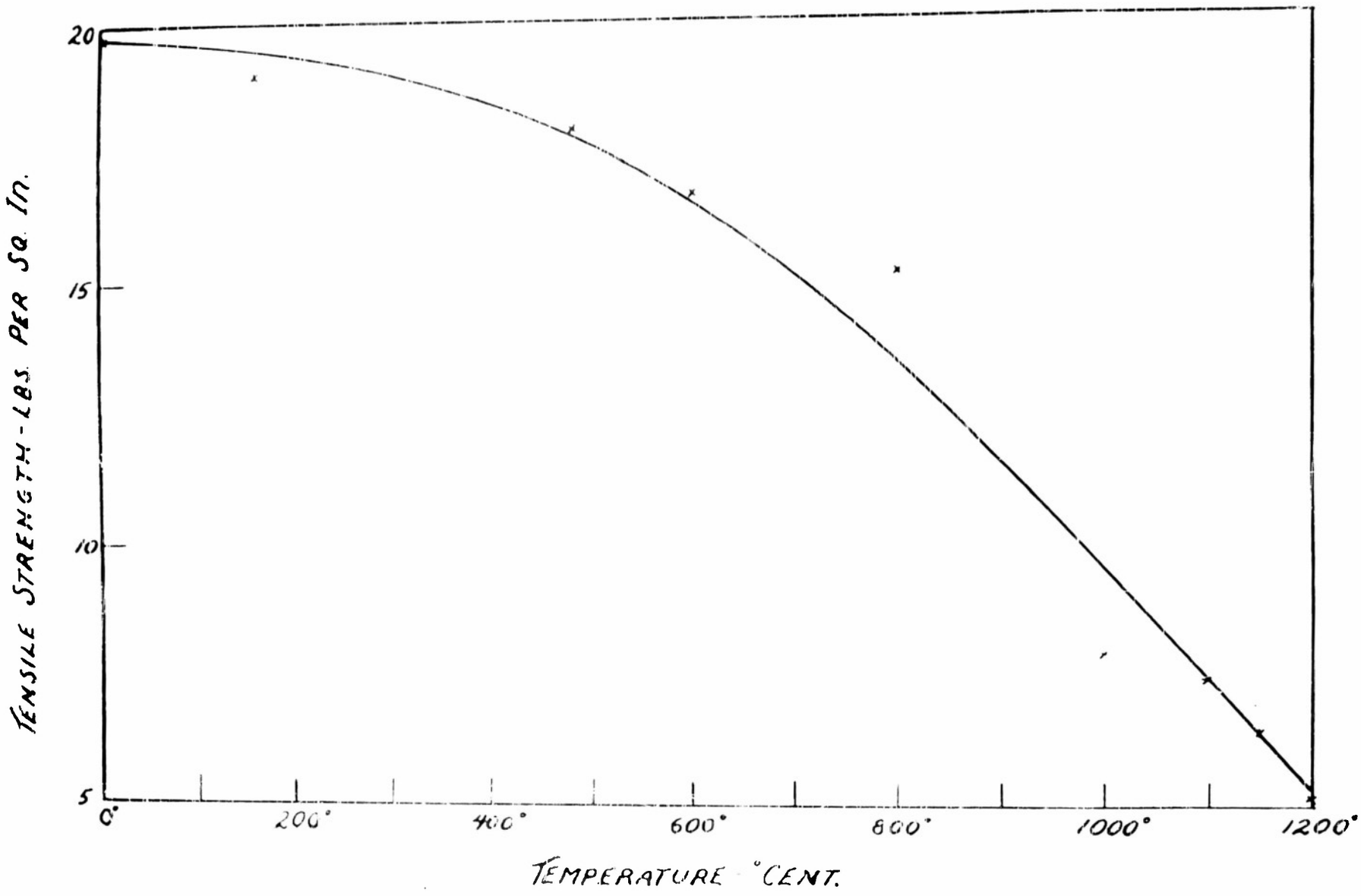

FIG. 16 TORSIONAL TENSILE STRENGTH CURVE.

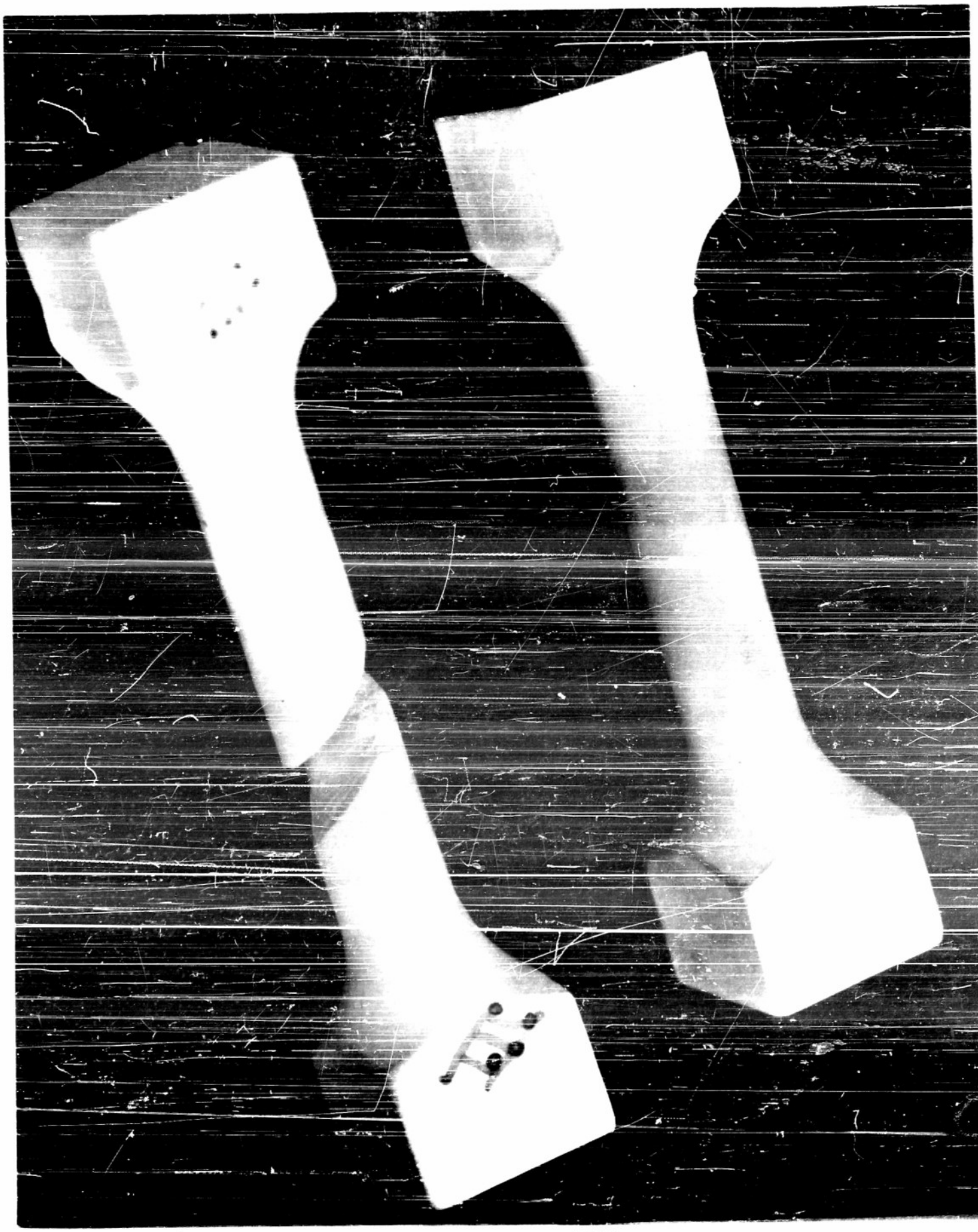

FIG. 17 FAILURE OF TORSIONAL SPECIMEN IN TENSION.

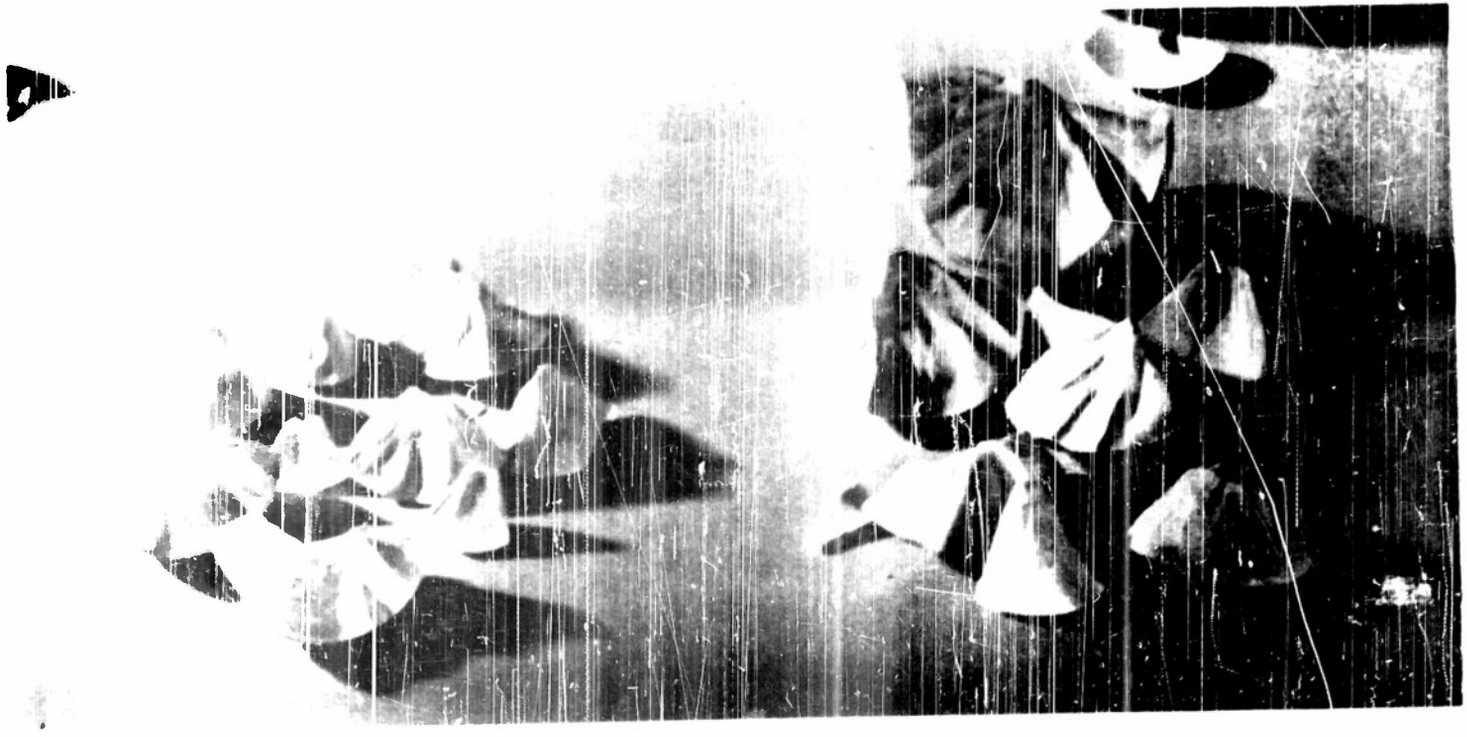

FIG. 19 TYPICAL HEATING FRACTURE OF SPHERE.

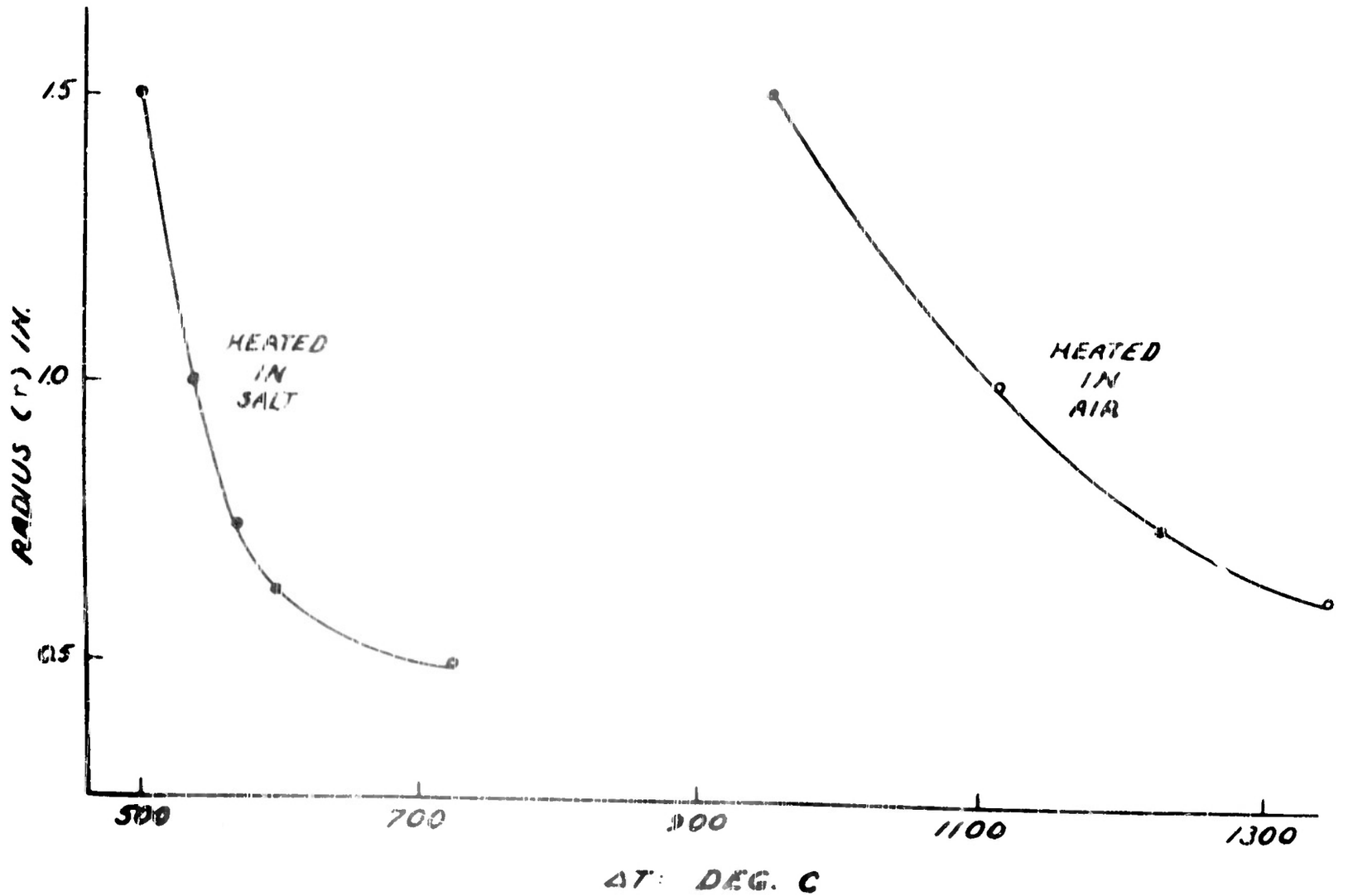

FIG. 20 RADIUS OF SPHERE VERSUS TEMPERATURE DIFFERENCE CAUSING FAILURE.

DISTRIBUTION LIST

(9) NavRes Lab., Tech. Info. Offr.

(1) NavRes Lab., Supt., Met. Div.

(2) ONR, Code 423

(1) ONR, N. Y.

(1) ONR, Rochester

(1) Phila. Naval Shipyard

(2) BuOrd - Re9

(1) BuOrd - Rec - 5

(2) BuOrd - Rex

(1) BuShips - 330

(2) BuShips - 336

(1) BuShips - 390

(2) BuShips - 433

(1) BuShips - 641

(1) BuShips - 660

(2) BuAer - AF - 41

(4) BuAer Gen. Rep.
Wright-Patterson Fld.

(2) Dept. of Air Force

(2) Dept. of Army, Ordnance

(2) Sig. Corps Eng. Lab.,
Fort Monmouth

(1) Dept. of Army, Signal Corps,
SIGET 1-5

(2) Univ. of Chicago, Metals Inst.

(1) M. I. T. Insulation Research

(1) Penna. State Coll., C. C. Henry

(1) Univ. of Illinois, Ceramics

(1) United Kingdom Sci. Mission
Washington, D. C.

(1) Amer Electro Met Corp, G. Stern

(1) Met. Res. & Dev. Co.

(1) Ohio State Univ., Res. Found

(1) Rutgers Univ., Ceramics

(1) Aunour Res. Found., Ceramic Div.

(1) Battelle Memorial, Director

(1) Battelle Memorial, R. W. Dayton

(1) M. I. T., Prof. Norton

(1) Calif. Inst. Tech., Jet Prop. Lab.

(1) M. I. T., Prof. Gaudin

(1) Rutgers Univ. Air Force Proj.

(1) M. W. Kellogg Co., Jersey City

(1) Norton Co., Worcester, Mass.

(1) GE, West Lynn, Mass.

(1) Westinghouse Elec., Phila.

(1) R.W.B. Corp., Santa Monica

(1) Allis Chalmers, Milwaukee

(1) Westinghouse Elec., Atomic Power
Div., Pittsburgh

(1) National Bu. Standards, Cer. Div.

(1) Argonne Natl. Lab.

(5) AEC, Tech. Inf. Director

(1) AEC, Metallurgy Branch

(1) Oak Ridge Natl. Lab., Metallurgy
Div.

(1) Oak Ridge Natl. Lab. C. E. Ellis

(1) Linde Air Prod., J. H. Gaines

(1) Pratt & Whitney Air craft,
E. Hartford 8, Conn.

(1) Flight Research Lab. Wright -
Patterson Fld.

(1) Metallurgical Research
Washington 6, D. C.

(1) Kennametal, Inc. Latrobe, Penn.

DISTRIBUTION LIST (CONT.)

(1) Wright Air Development Center
Patterson Fld.

(1) M. I. T. - W. D. Kingery

(1) National Bureau of Standards -
S. Levy

(1) R. P. I. - Prof. George H. Lee

(1) M. I. T. - Prof. R. L. Besplinghoff

(1) AEC - Ames Laboratory - Technical Librarian

(1) Argonne National Laboratory Info. Div.

(5) ASTIA - Dayton, Ohio